



UNIVERSITY OF LEEDS

This is a repository copy of *Impact of a pre-existing transverse drainage system on active rift stratigraphy: an example from the Corinth Rift, Greece*.

White Rose Research Online URL for this paper:  
<http://eprints.whiterose.ac.uk/149270/>

Version: Accepted Version

---

**Article:**

Somerville, DJP, Mountney, NP [orcid.org/0000-0002-8356-9889](https://orcid.org/0000-0002-8356-9889), Colombera, L [orcid.org/0000-0001-9116-1800](https://orcid.org/0000-0001-9116-1800) et al. (1 more author) (2020) Impact of a pre-existing transverse drainage system on active rift stratigraphy: an example from the Corinth Rift, Greece. *Basin Research*, 32 (4). pp. 764-788. ISSN 0950-091X

<https://doi.org/10.1111/bre.12396>

---

© 2019 The Authors. *Basin Research* © 2019 John Wiley & Sons Ltd, European Association of Geoscientists & Engineers and International Association of Sedimentologists. This is the peer reviewed version of the following article: Somerville, DJP, Mountney, NP, Colombera, L, Collier, REL. Impact of a pre-existing transverse drainage system on active rift stratigraphy: An example from the Corinth Rift, Greece. *Basin Res.* 2019; 00: 1– 25. <https://doi.org/10.1111/bre.12396> , which has been published in final form at <https://doi.org/10.1111/bre.12396>. This article may be used for non-commercial purposes in accordance with Wiley Terms and Conditions for Self-Archiving. Uploaded in accordance with the publisher's self-archiving policy.

**Reuse**

Items deposited in White Rose Research Online are protected by copyright, with all rights reserved unless indicated otherwise. They may be downloaded and/or printed for private study, or other acts as permitted by national copyright laws. The publisher or other rights holders may allow further reproduction and re-use of the full text version. This is indicated by the licence information on the White Rose Research Online record for the item.

**Takedown**

If you consider content in White Rose Research Online to be in breach of UK law, please notify us by emailing [eprints@whiterose.ac.uk](mailto:eprints@whiterose.ac.uk) including the URL of the record and the reason for the withdrawal request.



[eprints@whiterose.ac.uk](mailto:eprints@whiterose.ac.uk)  
<https://eprints.whiterose.ac.uk/>

# **Impact of a pre-existing transverse drainage system on active rift stratigraphy: an example from the Corinth Rift, Greece**

David J. P. Somerville<sup>1</sup>, Nigel P. Mountney<sup>1</sup>, Luca Colombera<sup>1</sup>, Richard E. Ll. Collier<sup>2</sup>

<sup>1</sup> *Fluvial & Eolian Research Group, University of Leeds, School of Earth and Environment*

<sup>2</sup> *Basin Structure Group, University of Leeds, School of Earth and Environment*

Corresponding Author: Somerville, D. J. P. eeds@leeds.ac.uk

## **Abstract**

Models to explain alluvial system development in rift settings commonly depict fans that are sourced directly from catchments formed in newly uplifted footwalls, which leads to the development of steep-sided talus-cone fans in the actively subsiding basin depocentre. The impact of basin evolution on antecedent drainage networks orientated close to perpendicular to a rift axis, and flowing over the developing hangingwall dip slope, remains relatively poorly understood. The aim of this study is to better understand the responses to rift margin uplift and subsequent intrabasinal fault development in determining sedimentation patterns in alluvial deposits of a major antecedent drainage system. Field-acquired data from a coarse-grained alluvial syn-rift succession in the western Gulf of Corinth, Greece (sedimentological logging and mapping) has allowed analysis of the spatial distribution of facies associations, stratigraphic architectural elements and patterns of palaeoflow. During the earliest rifting phase, newly uplifted footwalls redirected a previously established fluvial system with predominantly southward drainage. Footwall uplift on the southern basin margin at an initially relatively slow rate led to the development of an overfilled basin, within

which an alluvial fan prograded to the southwest, south, and southeast over a hangingwall dip-slope. Deposition of the alluvial system sourced from the north coincided with the establishment of small-scale alluvial fans sourced from the newly uplifted footwall in the south. Deposits of non-cohesive debris flows close to the proposed hangingwall fan apex pass gradationally downstream into predominantly bedload conglomerate deposits indicative of sedimentation via hyperconcentrated flows laden with sand- and silt-grade sediment. Subsequent normal faulting in the hangingwall resulted in the establishment of further barriers to stream drainage, blocking flow routes to the south. This culminated in the termination of sediment supply to the basin depocentre from the north, and the onset of underfilled basin conditions as signified by an associated lacustrine transgression. The evolution of the fluvial system described in this study records transitions between three possible end-member types of interaction between active rifting and antecedent drainage systems: (i) erosion through an uplifted footwall, (ii) drainage diversion away from an uplifted footwall, (iii) deposition over the hangingwall dip-slope. The orientation of antecedent drainage pathways at a high angle to the trend of a developing rift axis, replete with intrabasinal faulting, exerts a primary control on the timing and location of development of overfilled and underfilled basin states in evolving depocentres.

**Keywords** Gulf of Corinth, alluvial fan, rift basin, antecedent river, conglomerate.

## 1. Introduction

The onset of extensional faulting and associated rift-basin subsidence commonly trigger the accumulation of conglomerate and sandstone bodies, many of alluvial origin

(Graham et al., 2001; Martins-Neto & Catuneanu, 2010; Zaghloul et al., 2010; Hemelsdaël et al., 2017; Teixeira et al., 2018). In the continental realm, conglomerate bodies that form the initial fill of evolving rift basins typically record sedimentation from alluvial fans, and commonly transition up-section into fluvio-lacustrine deposits (cf. Sinclair et al., 1994; Graham et al., 2001; Zaghloul et al., 2010; Turner, 2010). Newly uplifted footwalls are prone to denudation by erosional processes and source these earliest syn-rift deposits (Mack & Leeder, 1999). This denudation is most notable where the impact of antecedent drainage is relatively subdued, and either rifting does not crosscut major drainage networks or fluvial systems are diverted away from the rift zone, for example by growing rift shoulders (Gawthorpe and Leeder, 2000). Where extensional regimes evolve at a high angle relative to pre-existing drainage networks, coarse-grained sedimentary deposits typically accumulate downstream of the point where drainage networks are sourced over, or deflected around, the newly uplifted footwall (cf. Gupta et al., 1999; Hemelsdaël et al., 2017; Hopkins & Dawers, 2018). Although newly developed normal faults are known to act as buffers to drainage over the hangingwall dipslope (Leeder & Jackson, 1993; Gawthorpe & Leeder, 2000), limited research has been undertaken to date to compare subsequent deposition on the hangingwall dipslope to their footwall-sourced counterparts.

The Corinth rift, Greece (Fig. 1), provides a location to study the impact of antecedent drainage on deposition over the hangingwall dipslope during the onset of rifting. Alluvial-fan deposits dominated by coarse grained, clast- to matrix-supported conglomeratic bodies are exposed in cliff faces – notably along valley sides – as part of an uplifted footwall block on the northern coast of the Peloponnese (Ford et al., 2013; Ford et al., 2016; Gawthorpe et al., 2017). Exposures of sedimentary successions

juxtaposed against normal faults allows for the detailed examination of sedimentary processes in a single fault block during the early syn-rift, and the impact of intra-basinal faulting on the prevalence of “overfilled” and “underfilled” depositional conditions (Gawthorpe & Leeder, 2000).

The aim of this study is to establish a depositional model to account for the generation of the early syn-rift conglomerate units deposited from antecedent drainage flowing over a hangingwall dip slope, and to describe the sedimentological variations that occur across the newly formed depocentre. Specific objectives of this research are as follows: (i) to map lithofacies variations of an alluvial fan sourced over the hangingwall dip slope of an evolving rift basin through space and time; (ii) to determine the processes by which sediment was transported and deposited by an alluvial fan present in the rift basin; (iii) to show how the alluvial-fan system responded to fault block rotation and local uplifted footwall blocks; and (iv) to propose palaeogeographic models that describe the depositional processes occurring in the basin from rift initiation to the present day.

These analyses are novel, significant and of broad appeal because they allow for the sedimentological history of a developing rift basin to be reconstructed in detail. The outcome of this study demonstrates the following key insights: (i) the benefits of underpinning tectonostratigraphic analyses with detailed sedimentological observations; (ii) the importance of antecedent drainage direction in the prediction of the distributions of alluvial facies and architectures in a single extensionally faulted block; (iii) the influence of subsequent intra-basinal faulting in the switching between

high sediment supply to accommodation ratios, and low sediment supply to accommodation ratios (i.e. “overfilled” and “underfilled” scenarios).

## 2. Geological setting

### 2.1. The Gulf of Corinth

The Gulf of Corinth is an area of active extension between the Peloponnese and mainland Greece. It formed as a result of extension associated with the subduction of the African tectonic plate underneath the Aegean Sea plate (forming the Hellenic Arc) to the west and south of the gulf (Doutsos et al., 1988; Bell et al., 2009). Prior to the onset of extension, a NNW-SSE trending fold-and-thrust belt, the Pindos thrust sheet, formed during the Late Eocene (Skourlis & Doutsos, 2003). This feature now forms the pre-rift basement, and the associated tectonic evolution originally separated the pre-existing drainage into a series of north-south orientated catchments that drained predominantly towards the north (Seger & Alexander, 1993; Zelilidis, 2000). Each catchment eroded the same Pindos thrust sheet, which is composed of Mesozoic carbonates and sandy clastic turbidites deposited on a passive margin and orogenic wedge (Degnan & Robertson, 1998). Rifting commenced in the Pliocene (Ford et al., 2016; Nixon et al., 2016) with the principal trend of the developing rift striking east-west, at high angle to the direction of antecedent drainage (Fig. 1; Collier & Gawthorpe, 1995). Rifting has continued to the present day and covers an area of approximately 105 km x 30 km (Fig. 1). Current extension rates vary from 10 to 16 mm/yr (Nixon et al., 2016), with higher rates in the west of the rift (Ford et al., 2016). Initial rifting led to the development of northward-dipping extensional faults on the northern coast of the Peloponnese.

Extension has progressively migrated to the north, with more recent faulting in the last 400 kyr (Gawthorpe et al., 2017) having occurred in the hangingwalls of older structures to form the morphology of the present-day Gulf (Ori, 1989; Ford et al., 2013). As a result, Plio-Pleistocene syn-rift successions up to 3 km thick, and of mixed continental and marine origin, are now exposed onshore as uplifted footwalls (Gawthorpe et al., 2017). Offshore in the present-day Gulf, sedimentary successions up to 2.5 km thick have accumulated as the Late Pleistocene and Holocene fill of rift basins. Both sets of successions record sedimentation in a variety of environmental settings, including continental, shallow-marine and deep marine environments (Nixon et al., 2016). Due to the relatively short extensional history of the rift and the lack of subsequent overprinting by other structural regimes, this area is especially well suited to the study of both onshore and offshore syn-rift sedimentation in settings adjacent to active extensional faults (Bell et al., 2009).

Syn-rift sedimentation occurred in two distinct phases: the first from the Pliocene to the Middle Pleistocene (400 ka), and the second from the Middle Pleistocene to the Present (Esu & Gerotti, 2015). This study focuses on the nature of sedimentation in the latter part of the first phase, during which depocentres hosted deep-water lacustrine systems with water depths of 300-600 m, indicated by deltaic foreset stratal packages that are several hundred metres thick (Gawthorpe et al., 2017) in the east (from the Alkonyides Gulf extending to the town of Selianitika; Fig. 1). These deltaic deposits pass into continental environments to the west (west of Selianitika) (Ford et al., 2013; Ford et al., 2016; Gawthorpe et al., 2017). The sedimentology of these palaeoenvironmental settings provides a record of both axially derived deposits that fed into Lake Corinth to the east (Ford et al., 2016; Gawthorpe et al., 2017), and transverse drainage systems

that resulted in deposition of sediment over relic uplifted footwalls (Collier & Dart, 1991).

As extension progressively migrated northward, the oldest stratigraphic intervals recording syn-rift sedimentation were progressively uplifted into the footwalls of younger faults, thereby resulting in the exhumation and exposure of older sedimentary successions of deep-water, deltaic and alluvial origin – from east to west, respectively (Dart et al., 1994; Ford et al., 2016). Large, Gilbert-type deltaic deposits are present across exposed cliff sections from Xylokastro to Aigio (Fig. 1; Collier & Dart, 1991; Dart et al., 1994). These fan deltas were sourced from feeder valleys that cut down through uplifting footwalls, or which exploited topographic lows between fault tips (Leeder & Jackson, 1993). Presently, over 1000 m of continental syn-rift deposits are exposed in a series of cliff faces up to 600-m high and hills in the footwall of the Psathopyrgos fault, directly west of Aigio (Fig. 1) (Bell et al., 2009).

## 2.2. The Profitis Elias Group

The early-rift deposits between Aigio and the Patras Rift are dominantly represented by the older Profitis Elias Gp. and the younger Galada Gp., both of which are well preserved in the Panachaikon fault block, a 7-8 km-wide unit between the Rion Strait and the Panachaiko mountain, where these two groups attain a combined thickness of 1.4 km (Palyvos et al., 2007; Ford et al., 2016). The Profitis Elias Gp. contains three formations of similar age: the Rodini Formation (west), the Salmoniko Formation and the Synania Formation (east), which are interpreted by Ford et al. (2016) to represent alluvial fan, braided stream and lacustrine environments, respectively. These formations record a

progressive fining in mean sediment calibre from west to east (Palyvos et al., 2007, Palyvos et al., 2010). The main focus of this study is the Rodini Fm., deposited furthest to the west on the northern tip of the Peloponnese.

Together, the three formations represent the major proportion of the Profitis Elias massif and attain a preserved (post-uplift) thickness of up to 600 m (Esu & Gerotti, 2015), with original depositional thickness estimated at over 1000 m (Ford et al., 2016). Multiple wadis expose the formations, where erosion over the last 400 kyr has left a reduced thickness (~10 m) of sandy siltstone of the Synania Fm. at the highest points of the massif, overlying large cliff faces that are 50 to 120 m high and which expose sections of the underlying Rodini Fm.

The Rodini Formation has not been the focus of prior detailed study; the majority of prior research efforts in the Gulf of Corinth region have focussed on the eastern parts of the rift (see Collier & Dart, 1991; Collier & Gawthorpe, 1995; Rohais et al., 2007). Previous studies of the Rodini Fm. are based on limited and fundamental observations of lithology over the area (see Doutsos et al., 1988; Esu & Gerotti, 2015; Ford et al., 2016), where the Rodini Fm. is present in the form of reddish to grey conglomerates dominated by cobbles and boulders. These deposits have previously been interpreted as the depositional record of an alluvial or fluvial system sourced from the north (Doutsos et al., 1988; Gawthorpe et al., 2017). However, this general interpretation needs to be refined through the development of a detailed palaeoenvironmental reconstruction based on analysis of lithofacies, sedimentary architectures, and on analysis of the spatial and temporal distribution of palaeocurrent data. These interpretations are the focus of this study, which is based on a detailed field-acquired data set.

### 3. Data and Methods

#### 3.1. Lithological mapping

Mapping was undertaken to document lithological variations across the study area, based on the three main rock types present: conglomerate, sandstone and siltstone. In addition to regional mapping, 37 sites were selected for detailed study; for these sites proportions of lithologies were recorded as percentages. Two hundred dip and strike readings (from 20 of the 37 sites), ranging from 04-40° dip angle, were separated into three groups of equal size based on their relative elevations and their magnitudes. This allowed the relative chronostratigraphic positions of the different sites to be determined.; in conjunction with lithological data, a tectonostratigraphic framework was then established (see Section 3.3. for detail).

For conglomerate lithologies, the percentage volume of both matrix and clasts was recorded to map subtle variations in lithofacies across the study area. The matrix of conglomerate lithofacies is defined as grains from clay to medium-sand size (similar to the procedures implemented by Steel & Thompson 1983; Sohn et al., 1999; Kim & Lowe, 2004; Puy-Alquiza et al., 2017, in their studies of alluvial deposits). The maximum grain size of the matrix, and minimum clast size of the overall deposit, define a bimodality in grainsize.

#### 3.2. Vertical profiles

Twenty of the 37 locations were chosen for detailed sedimentological analysis based on the description of vertical profiles at the decimetre scale (Fig. 2). Special attention was dedicated to detailing clast fabric and texture variations in conglomeratic bodies by tabulating individual clast features. Lithofacies were tabulated recording their thicknesses and key sedimentological features (e.g., grading, sedimentary structures, clast-to-matrix proportions). Profiles were placed in their approximate chronostratigraphic positions through extrapolation by combining observations of tectonic dip and topographic data (see below). There is no biostratigraphic control within the Rodini Fm., and there is no clear opportunity to establish an event stratigraphy, for example via radiometric dating. In total, twenty vertical profiles with a cumulative thickness of 250 m were recorded in detail.

These data were supplemented by an additional six large-scale log profiles recorded to capture larger-scale stratigraphic variations in lithology, through 533 m of the approximately 600-m-thick formation. These vertical profiles enabled the construction of a tectonostratigraphic framework for the area by combining them with data used for lithological mapping and structural data, as outlined above.

### 3.3. Tectonostratigraphy definitions

Establishment of the chronostratigraphy of the studied succession is problematic due to a lack of biostratigraphic control or of datable ash deposits similar to those found in syn-rift sediments to the east (Gawthorpe et al., 2017). To develop a well-defined tectonostratigraphy for the study area, bedding dip and strike data and topographic elevation were combined to determine the relative ages of deposits at different

localities across the study area, as a function of varying amounts of rift-induced differential tilting (Fig. 3). Depositional gradients are likely to have been low, given the absence of high-angle inclined foresets.. Small-scale intra-basinal faulting is also assumed to have minimal effect, with the few observed post-depositional faults experiencing throws of <5 m. This approach has allowed a tentative chronology of the deposits and has enabled establishment of a tectonostratigraphy with which to support interpretations of depositional environment, and of the influence of active faulting on palaeogeography.

The initiation of sediment accumulation is considered to have commenced in response to the onset of movement on the Panachaikon fault at 2.2 – 1.8 Ma (Fig. 4) (Gawthorpe et al., 2017). For this study, the rate of sediment supply is assumed constant, as the climatic and tectonic conditions of the inferred catchments for sediment delivery were persistent throughout the episode of sediment accumulation (Skourlis & Doutsos, 2003), leading to the definitions of timings outlined in this study. This is necessary in order to assign the sedimentary logs intervals recorded into their likely time episodes.

#### 3.4. Clast fabric and texture description

At each of the 20 sites where vertical profiles were recorded, conglomeratic facies were subject to detailed clast-fabric and texture analysis. At each site, up to two facies were chosen for clast measurements, and a square grid of 1 m<sup>2</sup> in area was placed on the outcrop surface. The 50 largest clasts within that square were characterised with respect to three qualitative attributes (composition, shape, roundness) and ten quantitative features (length, plunge and azimuth of three axes, from which

palaeocurrent direction was inferred based on identification of types of clast imbrication). These features were later corrected for bedding strike and dip. This approach was taken to randomise the clasts chosen for measurement, to obtain data in a systematic fashion, and to collect data for future studies on clast metrics. In total, 1,531 clasts were measured for these features from 10 conglomerate facies types; in addition, 1,001 palaeocurrent indicators were derived from patterns of clast imbrication. In this paper, focus is given to clast axis orientation data, composition data, and palaeocurrent data for the purpose of determining flow processes, sediment input sources and sediment flow directions over the basin. From clast composition alone, the detailed province cannot be determined given the presence of similar lithologies in the basement rocks on both sides of the basin. However, where information on clast composition is combined with clast-fabric analysis, an indication of palaeotransport direction (as indicated by clast imbrication) can be used to deduce the likely provenance for the basin-filling conglomerates.

## 4. Results

### 4.1. Lithofacies

Fifteen distinct lithofacies types are identified within the Rodini Fm: ten types of conglomerate and five types of sandstone and siltstone (Table 1; Fig. 5). In the conglomerate facies, clast composition is dominated by a mixture of well-sorted sandstone, well-cemented limestone, and metamorphosed sandstones and limestones. All clasts were apparently sourced from basement units (dominated by metamorphosed carbonates and flysch deposits; Skourlis & Doutsos, 2003) that formed the Pindos

Mountains to the north, or were uplifted in nearby footwalls. The distribution of lithofacies and architectural elements through the formation is represented by twenty vertical profiles (Figs. 6a, 6b, 6c) taken from across the study area (Fig. 1).

#### 4.2. Architectural Elements

Architectural elements are defined here as discrete packages of sediment with a measurable lateral and vertical extent (and associated 3D geometry), deposited as a result of a specific depositional process and its associated processes (for example, a braided fluvial channel deposit and its associated overbank sediments) (Fig. 7). Their comprising facies, in conjuncture with the elements themselves, form a specific set of arrangements (facies associations) leading to the interpreted natural progression of depositional environments described in sections 4.3. and 4.4.

##### AE1: Coarse non-cohesive debris flow elements

*Description:* This element type comprises 25.7% of the measured succession. Sedimentary units of this type range from 3 to 10 m thick and are dominated by beds that are laterally extensive over tens of metres, themselves each from 0.5 m to 5 m thick. Compared with other associations, beds exhibit lateral variations in thickness up to 0.5 m. The base of each element of AE1 is strongly erosional with 10 – 20 cm persistent relief. Basal erosion surfaces of these elements are overlain by a coarse boulder conglomerate bed (B-wtm, B-plm). Up-section, stacked beds of finer conglomerates (typically cobble to boulder grade) dominate. All beds are massive with no discernible internal stratification (B-wtm, B-plm, B-ple, C-rl). Beds contain a higher proportion of matrix (15 - 20%) than other architectural elements. Thin beds of finer facies (S-s) may

be present within the element, and are laterally extensive with a maximum thickness of 0.2 m. AE1 units may be stacked vertically, resulting in amalgamated conglomerate packages, or may occur as isolated elements separated by other types of architectural elements (AE3, AE4, AE5).

*Interpretation:* Structureless, matrix- to clast-supported conglomerates are most commonly the result of rapid deposition by non-cohesive debris flows that typically wane over time to deposit relatively more well-sorted and fining-up conglomerate beds up-section from hyperconcentrated flows (Nemec & Steel, 1984; Costa, 1988; Sohn et al., 1999; Went, 2005; Calhoun & Clague, 2018). Poorly sorted units with isolated boulders and a wide range of clast sizes are interpreted as the rapid freezing of coarse clasts within flows, with stacked sets and erosional bases to each bed. This indicates that flow events were frequent and initially erosive (Miall, 1996), and representative of more turbulent flow types (Blair & McPherson, 1994; Jo et al., 1997). These types of elements and their constituent lithofacies are typical of proximal alluvial-fan environments, notably in locations close to their feeder valley (Gloppen & Steel, 1981).

AE2: Coarse, poorly channelized streamflow units and associated waning-flood elements

*Description:* This element type comprises 35.0% of the measured succession. These associations are 2 to 17 m thick and are dominated by conglomerates and silty sandstones arranged into two or more beds, each of which is 0.2 to 3 m thick. Conglomerate beds are lenticular over distances of 5 to 10 m where outcrop extent permits characterisation, with finer-grained facies being more laterally extensive. Coarse-grained conglomerates with erosional bases (B-wtm, B-rlf) are overlain by normally graded conglomerates, either forming a single bed (B-rlf) or fining-upward

bedsets with multiple beds (B-rlf, C-rlf, P-wtm, G-wtm), which may be sharply overlain up-section by silt- and sand-grade facies (S-l, S-s, S-h). Conglomerates are compositionally and texturally mature, with a high (90-100%) clast proportion by volume. Fine grained units are dominantly massive. AE2 typically occur as stacked sets of unknown maximum thickness (due to outcrop limitations), but observed to be over 50 m, or interbedded with elements AE5 and AE1.

*Interpretation:* Moderately to well-sorted conglomerate units of texturally and compositionally mature clasts that fine upward are typical of bedload transport processes (Miall, 1996); deposits are subsequently represented up-section by sand and silt deposits representing the waning of floods (Maizels, 1993; Sohn et al., 1999). Decimetre- to metre-scale infilled scours show these events to be highly erosive and often rapid in nature (Jo & Chough, 2001; Collinson et al., 2006) where each element is taken as a single, or stacked set, of depositional events. In places, fine-grained facies show horizontal lamination picked out by subtle grain-size variations from silt to fine-sand, here speculatively interpreted as the expression of waning deposits during flood events (Gloppen & Steel, 1981; Sohn et al., 1999). The lozenge shape of the conglomerate beds in cross section, in conjunction with their stacking style, indicate elements of weak channelization (Khadkikar, 1999; Collinson et al., 2006) of coarse-grained bedload conglomerates (Miall, 1996). AE2 is interpreted as occurring on the medial section of an alluvial fan, and likely as a downstream expression of AE1.

AE3: Coarse, unchannelised flow elements

*Description:* This element type comprises 6.14% of the measured succession. These elements are at least 10 – 15 m thick and are composed of one sheet-like coset of conglomerate, divided internally into 0.5 m-thick horizontal beds delineated by

traceable surfaces (marked by a change in matrix grain size from fine sand to silt grade, and a reduction in clast frequency to 50% 10 cm either side of the surface) and clast orientation variations between beds. The elements are laterally extensive across outcrops and cliff sections at a minimum of 20 m, and have flat, sharp bases. Cobbles dominate and reach up to 15 cm in diameter, with a medium-sand-grade matrix (C-pth) forming up to 20% of the beds. Within horizontally stratified sets, clast long axes are typically flat-lying, parallel to stratification. Although AE3 elements are not common over the study area, where present they are bounded by AE1 elements at their base and top.

*Interpretation:* Repeated non-channelised flows lead to multiple stacked horizons of cobble-grade conglomerates being deposited (Gloppen & Steel, 1981; Mack & Leeder, 1999) where lateral continuity of units, a lack of grading, and lack of erosional bases, indicate a highly viscous rheology (Todd, 1989; Kim & Lowe, 2004). Deposition occurred in a relatively proximal setting within the fluvial system, likely close to a primary feeder valley of the alluvial fan, as indicated by the large cobble clast sizes that dominate throughout (North & Davidson, 2012). A high sediment load led to a traction carpet of clasts being deposited (Todd, 1989) and preferentially orientated with long axes parallel to bedding surfaces. A lack of fine-grained deposits in AE3 indicates that repeated events were of high magnitude and possibly of high frequency, allowing for consistent coarse-grained deposition with no time for the settling of sediment from suspension (Wells, 1984; Hwang et al., 1995).

#### AE4: Medial fan debris-flow elements

*Description:* This element type comprises 7.61% of the measured succession. These elements are typically 1.5 to 9 m thick, but may be thicker locally. They are formed by

1.5 to 4 m thick conglomerate beds which are laterally extensive across outcrops (~50 m). The thickness of each bed varies laterally by up to 50 cm, but does not pinch out. Each bed has an erosional base to underlying deposits of poorly sorted boulder conglomerates containing sand lenses (B-pll) or moderately sorted cobble conglomerate (C-rll), which together form the element. Repeated sandy-silt lenses are common throughout elements. Conglomerates are clast supported, varying from pebble to boulder grade (up to 30 cm in diameter) and have a fine silty-sand matrix making up 5-20% of the lithology. Beds in the element are massive; however, silty-sand lenses within B-pll and C-rll beds locally demonstrate trough cross-stratification on the decimetre scale with sets up to 20 cm thick. AE4 elements are typically deposited in association with AE1 and AE5 elements; larger AE4 elements are deposited subsequent to AE5 elements with a transitional boundary over several metres as the proportion of B-pll and C-rll facies increases. In some cases, smaller examples of AE4 elements occur nested within successions otherwise dominated by AE1 elements.

*Interpretation:* Ungraded conglomerates of poorly to moderately sorted clasts are commonly formed by cohesive debris flows (Lowe, 1979; Suresh, 2007) as sediment undergoes frictional freezing, subduing settling processes (Cronin et al., 2000). Sandstone formation displays rare weakly developed sets of trough cross-stratification possibly representative of juvenile unit bar development (as stratification does not extend through entire sand units where present) or 3D dune development (Gloppen & Steel, 1981; Reading 1996) during the later stages of flows. These units are largely reworked and partially eroded by further mass-flow events (Lindsey et al., 2005) leading to limited preservation.

AE5: Fan-toe sandstones settled from suspension (with upper plane-bed conglomerate lenses) elements

*Description:* This element type comprises 17.2% of the measured succession. These elements are 1 to 6 m thick and laterally persistent between outcrops. Internally, they are composed of sets of sandstones that are 0.2 – 2 m thick and conglomerate units that are 0.1 to 1 m thick. Fine-grained facies extend laterally for up to tens of metres (S-l, S-s), whereas conglomerate facies (B-ple, C-rl, P-wtm, G-wtm) are 2 to 5 m in width. Boundaries between sets (and the elements themselves) are sharp but not erosional. Fine-grained units are moderately sorted, whereas conglomerate facies are well sorted with little to no matrix (typically <5%) and contain texturally and compositionally mature (well-rounded) clasts; 98% of clasts are <5 cm in diameter (but up to 15 cm at certain locations). All beds are internally massive. Rare in-situ calcrete nodules are found close to the tops of some sandstone beds, and are typically 2 cm in diameter. These elements are interbedded with AE2, AE5, AE7, and rarely AE1 units, and are common across the study area.

*Interpretation:* Massive, structureless sands and silts are most commonly deposited from rapid suspension during waning hyperconcentrated flows (Nichols & Fisher, 2007; Köykkä 2011; Lewis et al., 2017) commonly observed on the distal sections of an alluvial fan. Pebble-grade conglomerate lenses within the units represent higher-energy upper plane-bed deposition (Jo & Chough, 2001) forming channelized pebble streams (Crocì et al., 2016). The maturity of the clasts, both texturally and compositionally, are representative of their increased distance from the sediment input source (Miall, 1996). Rare calcrete nodules in AE5 units are indicative of an arid or semi-arid climatic setting (Retallack, 2001; Alonso-Zarza, 2003), and a prolonged period of stability allowing calcrete formation in a silt-prone substrate (Alonso-Zarza, 2003).

#### AE6: Fan-toe overbank elements

*Description:* This element type comprises 6.18% of the measured succession. These elements are 0.5 to 5 m thick and laterally persistent between outcrops. They are composed internally of silty sandstone (S-s, S-h) and predominantly clayey lithologies (F) that are 0.2 to 2 m and 0.05 to 0.1 m thick respectively. Silty sandstones (S-s, S-h) are laterally extensive by tens of metres; however clayey units vary in thickness from 5 cm to 10 cm within the same bed. Bed boundaries are sharp, and the two lithologies alternate through the element. Silty sandstone beds are moderately sorted ranging up to medium sand; a marked colour change and sharp increase in clay proportions denotes change to finer lithology. Beds are dominantly massive, though with some millimetre-thick horizontal laminations at the top of some silty sandstone beds. These elements occur in larger packages tens of metres thick, in association with AE5 and AE2 elements.

*Interpretation:* Similar to AE5, sand and siltstone units represent deposition from suspension of waning flows (Nichols & Fisher, 2007; Köykkä 2011; Lewis et al, 2017). Thin clay horizons represent the end-of-flow deposition (both from tractional and suspension processes), and the development of palaeosols identified by their lateral continuity and a lack of further structure (Platt & Keller, 1992; Mack et al., 1993). Where AE6 and AE2 elements are found together, potential active channels are interpreted to have been abandoned through time and subsequently subject to low sedimentation rates, as active deposition occurs elsewhere on the fan (Davies & Gibling, 2010).

#### AE7: Shallow-lacustrine elements

*Description:* This element type comprises 2.21% of the measured succession. These elements attain thicknesses of 4 to 10 m and are laterally extensive for up to 20 m.

Elements are composed internally of 0.5 to 1 m beds of silty sandstone and conglomerate lithologies. Finer-grained units (S-sh) are laterally extensive over tens of metres, whereas conglomerates (P-wtm, G-wtm) typically pinch out laterally over 2 to 10 m. Silty sandstone beds contain small shell fragments such as *Melanopsis synaniae* and *Goniochilus achaiae*, freshwater gastropods (Esu & Gerotti, 2015); shell fossils are less than 2 cm in length and occur as shell beds intermittently within the element or single dispersed shells amongst the finer-grained lithofacies. Conglomerate facies are characterised by 1 to 5 cm diameter, well-rounded clasts and contain no matrix. Beds are mostly massive, but some contain shell horizons within beds and horizontal laminations. These elements do not appear to be preferentially associated with other architectural elements.

*Interpretation:* These elements are similar in origin to deposits of AE6; however, the presence of laterally persistent laminae deposited during steady suspension fallout conditions and the occurrence of freshwater shell fragments (outlined in Esu & Gerotti, 2015) testifies to the development of potential shallow lacustrine conditions (Abdul Aziz et al., 2003; Ford et al., 2016), associated with the inundation of the depocentre by Lake Corinth to the east and, later, the opening of the Rion Strait to the west (Gawthorpe et al., 2017).

#### 4.3. Chronostratigraphy

As a result of the Rodini Fm. being dominated by rapidly deposited conglomeratic units, absolute dating within the sediments is difficult due to a lack of potential data sources (Gawthorpe et al., 2017). Movement on major bounding faults to the south of the depocentre initiated at approximately 2.2 – 1.8 Ma (Gawthorpe et al., 2017) and this

activity likely generated the initial accommodation to allow for the onset of accumulation of the conglomerates of the Rodini Fm. Corals and shells found in the overlying Synania Fm. siltstones provide a biostratigraphic age of approximately 420-400 ka (biozone MNN20) (Palyvos et al., 2010; Esu & Gerotti, 2015) that delimits the end of the episode of accumulation of the Rodini conglomerates. Thus, the total time available for accumulation of the Rodini Fm. is 1.8 – 1.4 Myr and the proposed relative time periods in this study would each represent one third of that value (approximately 600 – 470 Kyr each, assuming constant accumulation rates). Thirds were chosen in order to show a clear chronostratigraphic progression of sedimentological features, while retaining as much accuracy as possible in the relative geological ages of each study site.

Bedding dips reflect both tectonic and sedimentological factors: (i) original rotation of the palaeotopography as activity on the main bounding fault to the south occurred, forming shallower dips up-section, (ii) post-depositional fault block rotation as extension became accommodated by new north-dipping faults to the north, increasing the dips of beds towards the south, and (iii) deposition predominantly occurred in an alluvial-fan setting, which results in a general decrease in depositional dip angles away from the fan-apex feeder valley. Dip angles vary between 6 and 40 degrees across the study area, with maximum dips recorded in the west and south (corresponding with lower elevations and earlier stratigraphy that has been subject to greater fault-induced post-depositional rotation), and minimum dips recorded to the east and in the centre of the study area (corresponding with higher elevations and later stratigraphy, with less fault-induced post-depositional rotation).

The integration of structural and topographic data allow for the definition of three relative time slices through the Rodini Fm. into which the study sites can be grouped (based on their locations within the study area). Sedimentological variations through both time and space can subsequently be defined and used to create an overall tectonostratigraphy in both dip and strike orientations (Fig. 8). A relative increase in the proportion of conglomerate deposits towards the margins of the depocentre through time, in conjunction with an increase in AE1 and AE2 architectural elements across the study area, indicates that the fan system prograded across the basin.

#### 4.4. Definition of tectonostratigraphy and the use of clast-fabric analysis

The prevalence of dominantly debris flow and flood-sourced architectural elements across the study area, as outlined in Figs. 6a, 6b and 6c, is consistent with the development of an alluvial fan. This is further supported by the facies themselves, with the fabric of many structureless, coarse conglomeratic units indicative of alluvial-fan flow processes (Table 1). The lack of well-developed sandy mesoforms of fluvial origin is notable..

Sedimentological data derived from vertical profiles, when placed within the outlined relative time frame, allow for tectonostratigraphic definition as outlined in Fig. 8. Clast orientations with respect to palaeoflow directions indicates flow processes: long axes parallel to palaeoflow suggest deposition by debris flows, whereas intermediate axes parallel to palaeoflow suggest deposition by streamflow (Major, 1998). On this basis, debris-flow deposition in an alluvial-fan environment apparently prevailed in the north of the study area and extended into the depocentre towards the south and east as

extension progressed. Streamflow processes (AE2) are predominantly recorded in the east and south, and their prevalence lessens through time as the alluvial fan prograded and subdued their depositional environment.

The nature of the hangingwall dip slope alluvial fan was progradational to the west into the Patras Rift, to the south towards smaller-scale alluvial fans sourced from the uplifted footwall of the depocentre, and advancing towards lacustrine-dominated depocentres to the east (represented by Synania Fm. deposits) (Fig. 9). The progradation is represented by the advancement of facies belts away from the feeder valley with time, interpretable from the overall coarsening up of facies in distal locations. Footwall-derived alluvial fans, indicated by larger clast sizes and increased clast angularity, in conjuncture with northward palaeoflow directions, were smaller. As the basin cuts the pre-rift drainage at high angle, the northward dipping fault develops small drainage catchments as footwall uplift occurs to feed into the basin dominated by south-flowing drainage over the hangingwall. Due to increased erosion of syn-rift units close to the Panachaikon footwall scarp, it is difficult to recognise the development of these smaller fans through time; it is likely that these alluvial fans increased in size due to continued denudation of the associated uplifted footwall (cf. Densmore et al., 2007; Mirabella et al., 2018; Pechlivanidou et al., 2018).

The sand and silt deposits of the Synania Fm., which overlies the Rodini Fm., are interpreted to represent a lacustrine incursion caused by the northward migration of faulting and accommodation generation (Ford et al., 2016). Observations of shells and shell horizons within the unit (Palyvos et al., 2007; Esu & Gerotti, 2015), and extensive deposits interpreted as shallow-lacustrine deposition (see AE7) support this. The major

sediment source from the north was eventually cut off by the formation of new normal faults, causing key sediment routeways from the north to be blocked, thereby shutting down the depositional system before the basin began to uplift over the last 400 Kyr.

## 5. Discussion

### 5.1. The impact of rifting on fluvial drainage

The architectural elements detailed in this study represent different parts of the gradual transition (from proximal to distal locations) down-system of a large alluvial fan; massive debris flows lead into normally-graded bedload conglomerates that decrease in frequency away from major sediment source points, counterbalanced by an increase in fine-grained facies. Towards the east, fine-grained units containing shell fragments represent the lateral facies transition to lacustrine-dominated systems.

Placing the detailed sedimentological vertical profiles in the context of relative time slices allows for the creation of palaeogeographic models detailing the evolution of the depocentre (Fig. 10). To the north of the present-day Gulf of Corinth, the River Mornos catchment drains the structurally quiescent Pindos Mountains (Piper et al., 1990) and forms an 8 x 4 km southward-prograding modern delta. This system is likely to be the ancestral fluvial system described in this study (the catchment of which has been inherited in the present day), and acted as the principal sediment source that fed the alluvial fan represented by the Rodini Fm. The fluvial system is interpreted to have flowed south-west, following the alignment of east to west propagating fold-and-thrust structures with a south-west to north-east strike. These were formed during the Early

Oligocene to Late Eocene (Underhill 1989; Skourlis & Doutsos, 2003), and were also exploited by other antecedent drainage systems in the Gulf (Gawthorpe et al., 1994). As the fold-and-thrust structures form topographic highs between catchments, subtle variation in topographic dips between structures allow for the switching of dominant drainage direction from north to south across the elevated highs (Gawthorpe et al., 2017).

Rifting propagated through the catchment at high angle, with the major northward-dipping master fault uplifting pre-rift basement to the south of the study area and forming a barrier to flow. As the hangingwall subsided, accommodation was created and an alluvial fan began to build out into the depocentre as flows spread radially to fill the available accommodation and attain an equilibrium profile. This process is interpreted to have continued until a new master fault developed in the north and acted to uplift the depocentre, and as a new footwall created a barrier to sediment pathways, sediment supply ceased and caused the exposure and erosion of the Rodini Fm. to the present day.

This interpretation represents one of three possible end-member scenarios whereby a rift system cuts a large-scale drainage catchment, examples of which are found across the Gulf of Corinth. The three evolutionary scenarios are explained below.

(i) Drainage incision keeps pace with footwall uplift; flow is orientated in the same direction as the dip of major normal faults. Erosion down into the bedrock lithology forms valleys in the footwall and eroded sediment is deposited directly into the newly formed depocentre (see Bentham et al., 1991; Backert et al., 2010; Leeder et al., 2012; Hemelsdaël et al., 2017).

(ii) Drainage is diverted away from the uplifting footwall; flow is orientated in the same direction as the dip of major normal faults, however a combination of low erosive power and bedrock resistance to erosion (Allen & Densmore, 2000) results in the diversion or complete reversal of drainage away from uplifted sections (see Rohais, 2007; Gawthorpe et al., 2017). Small catchments form on the uplifted footwall close to the fault face, forming relatively small, high-gradient fans and fan deltas along the length of the fault (Gawthorpe et al., 1994).

(iii) Drainage flows over the hangingwall dipslope; flow is orientated in opposite direction to dip of major normal faults. This causes wider, lower-gradient fans and deltas. Sediment yield is influenced by antecedent catchment parameters (in conjunction with a dominant tectonic uplift control), such as bedrock lithology and climate, which are not influenced by the evolving rift system (described in detail in this study; see further examples in Mack & Seager, 1990; Martini & Sagri, 1993). Experimental work by Clarke et al. (2010) studying alluvial fan development with a downstream boundary condition (such as a fluvial system preventing progradation, or structural barrier) found that initial deposition from sheet-like (i.e. non-confined) flows developed to channelized flows with time and advancement of the fan. In this study, the Panachaikon fault provides a boundary condition, and early deposits of the Rodini Fm. representing possible sheet-like flows (see Figure 6a, log L1) transitioning up-section into proposed channelized flow sediments (see Figure 6a, log L3) indicating a subduing of autogenic fan cycles of deposition (van Dijk, 2012).

These end-members have been explored previously (Gawthorpe et al., 1994; Gawthorpe & Colella, 2009); however few studies focus on intrabasinal faulting acting as barriers to hangingwall dipslope routes of sediment transport. Although scenario (iii) is described

in detail in this study (and can be supported by the pattern of local sedimentation within the depocentre), Fig. 10 shows that conditions allowing for scenarios (i) and (ii) to occur were present between the initiation of extension and the present day if considering this sub-basin in a regional context. The Trizonia fault to the northeast, located under the present day Gulf and likely active at the same time as the Panachaikon fault (Ford et al., 2016) may have provided a barrier to the Mornos drainage and diverted the system over the hangingwall dip slope of the Panachaikon fault – scenario (ii). Following deposition of the Rodini conglomerates, initiation of the Marathias (see Fig. 1) and Psathopyrgos faults at approximately 400 ka (Palyvos et al., 2010) has led to a marked increase in extension rates in the modern Western Gulf (Ford et al., 2016; Gawthorpe et al., 2017). This has developed more pronounced graben conditions with a northern basin-bounding fault (the Marathias fault, see Fig. 10) (Beckers et al., 2015) of which the uplifted footwall is eroded sufficiently by the Mornos fluvial system to allow the formation of a modern fan-delta depositing directly into the hangingwall – representing scenario (i). A significant novel outcome of this study is that the succession records evidence that all three scenarios can be present during the life cycle of a single fault block depending on the presence and activity of intrabasinal faulting.

The results of this study demonstrate the effect of a downstream boundary condition (in this case, an uplifted footwall) on alluvial-fan deposition. Numerical modelling studies (e.g. Van Dijk et al., 2012; Clarke et al., 2010; Clarke, 2015) commonly focus on the autogenic development of fan systems and surface depositional processes. Results from this study can be incorporated into future models to provide more realistic structural settings for alluvial-fan development, which will aid in the study of alluvial system response to fault development and basin subsidence for a variety of scenarios (e.g.,

analysis of the effect of differing rift and drainage orientations). Comparing results from such modelling efforts to real-world studies of ancient outcropping successions (this study), and similar modern analogues (e.g., the Okavango delta – a large alluvial fan oriented perpendicular to the trend of active rifting) will markedly increase our understanding of sedimentary system response to active faulting at a variety of scales.

## 5.2. The Rodini Fm. in the wider context of the Gulf of Corinth

Across the uplifted footwall exposures of the northern Peloponnesos, multiple different syn-rift depositional environments are represented. In the east near Corinth, sediments are dominated by fan deltas and deep-marine deposits of the ancient Lake Corinth, within the depocentre of the now uplifted footwall (Doutsos & Piper, 1990); these deposits transition up-section into shallow-marine sands related to the transition from the lake to the modern day Gulf (Rohais et al., 2007a; Ford et al., 2016). Further to the west towards the study area, the influence of continental sedimentation becomes apparent in the hangingwalls of the Kalavryta and Demestika Faults (Hemelsdaël et al., 2017) and in the study area of this paper, where conglomeratic deposition represents alluvial-fan and possible braided-stream environments. Gawthorpe et al. (2017) show that the uplifted sections exposed today can be separated into two distinct rift phases; the first where extension is localised around Corinth and extends as far west as Aigio (5.0-3.6 Ma to 2.2-1.8 Ma), and the second where extension has begun in the study area on the Lakka and Panachaikon faults (allowing the deposition of the Rodini Fm.), north of Corinth (2.2-1.8 Ma to present). Within this second phase, the initiation of the Psathopyrgos fault on the present day coastline uplifts the Rodini Fm. and causes the opening of the Rion Strait. This period has been narrowed down to approximately 400

ka by dating of overlying shell fauna in the Synania Fm. (Palyvos et al., 2007; Esu & Gerotti, 2015) which was deposited during a period of simultaneous activity on both the major Panachaikon Fault and Psathopyrgos Fault (Fig. 10).

In the outlined first rifting phase, similar deposits to those found of the Rodini Fm. are found in the hangingwalls of the Kalavryta and Demestika Faults. Hemelsdaël et al. (2017) outlined the tectonosedimentary evolution of these deposits and found multiple similar facies and facies associations to those outlined in this paper; similar units of coarse boulder conglomerates deposited close to a dominant sediment input source, transitioned distally to finer-grained sands and siltstones. The drainage system leading to the deposition of the facies described by Hemelsdaël et al. (2017) differs from the one described herein in two key ways; (i) although orientated at high angle to fault strike, antecedent drainage and flow is over the footwall and keeps pace with the uplifting bedrock, depositing sediment directly into the newly formed depocentres, and (ii) the drainage system as a result cuts across multiple fault blocks, where older normal faults to the north are buried by syn-rift sediments. It is inferred that similarly high sediment supply through one dominant sediment input source prevailed. This, in combination with both drainage catchments eroding similar bedrock (due to the inherited palaeotopography around Kalavryta being dominated by the same Pindos Units forming the bedrock lithologies of the Mordos catchment (Degnan & Robertson, 1998)), leads to strikingly similar deposits in these two depocentres at different times. In the Prinos and Tsivios fault blocks, coarse basal conglomerates of interpreted alluvial origin, fill in the palaeotopography, in a very similar manner to the one documented herein for the Rodini Fm.

To the west of the Panachaikon fault hangingwall, the Patras rift extends towards the south-west, having initiated on an extensive low-angle listric fault which underpins extension in the Gulf of Corinth (Sorel, 2000). The rifts are linked by two transfer fault zones trending towards the north-east, on the western end of the Panachaikon fault (Flotté et al., 2005). Imbricated cobbles within the Rodini Fm. indicate that part of the river drainage was directed into the Patras rift axially, as the uplifted footwall of the Panachaikon fault acted as a buffer to flow. The sediment supply likely outpaced the formation of an accommodation zone between the differently orientated rift segments (Morley et al., 1990) allowing for the continued progradation and deposition of fluvio-alluvial deposits into the Patras rift (Doutsos et al., 1988). This is similar to other locations in the Gulf of Corinth where steep-sided Gilbert fan deltas would build into both the ancient Lake Corinth and the more recent Gulf (Rohais et al., 2007; Rohais et al., 2008; Backert et al., 2010), across multiple hangingwall depocentres each with varying amounts of accommodation space.

Following deposition of coarse alluvial conglomerates in the study area, the initiation of the Psathopyrgos fault (Fig. 1) formed a hangingwall depocentre north of the fault. Sediment supply into the hangingwall of the Panachaikon fault was subsequently shut off; hence during the period of simultaneous activity on the Panachaikon and Psathopyrgos faults, deposition of coarse-grained units was unable to cross over the faults to provide a linkage between depocentres. This is a direct result of drainage being orientated to flow over the hangingwall dip slope as opposed to the uplifted footwall. In both scenarios, younger faults are orientated in the same direction as their predecessors.

## 6. Conclusions

1. The Rodini Fm. is characterised by a 600 to 800 m-thick succession of upward coarsening conglomerates (up to ~75 cm clast sizes) with subordinate finer-grained lithologies. The succession represents the accumulated deposits of a major prograding alluvial-fan system. In western locations, stacked elements of boulder-to-cobble grade conglomerates represent proximal debris-flow and hyperconcentrated-flow deposits. In central and southern locations, distal to sites of major sediment input, conglomerates fine to pebble- and granule-grade, and the proportion of sand-grade and silt-grade facies increases significantly. Further to the east and up-section, a lacustrine influence is recorded by the occurrence of siltstone units containing a lacustrine shelly fauna.

2. Palaeocurrent data collected from 20 study sites (1,001 measurements total) indicate a dominant major sediment input source from the north of the study area flowing south over the hangingwall dip slope of the Panachaikon fault, a major basin-bounding fault. This alluvial system likely inherited the ancient course of the Mornos River and its catchment.

3. The uplifted footwall of the Panachaikon fault acted as a barrier to the Mornos catchment, and subsequently diverted drainage into adjacent depocentres to the east (ancient Lake Corinth) and west (Patras rift).

4. Palaeocurrent data indicating northerly flow, close to the uplifted footwall of the Panachaikon fault, indicate footwall-derived sediment deposition occurred in the basin on a small scale at both the fault tip of the Panachaikon fault to the west, and the point

of hard linkage between the Panachaikon and Lakka faults. These areas were exploited by small drainage catchments eroding the uplifted footwall.

5. The initiation of the Psathopyrgos fault to the north at approximately 400 ka provided a barrier to flow over the Panachaikon fault hangingwall. Simultaneous extension on both of these faults induced an episode of rapid basin subsidence that resulted in an initially lacustrine transgression over the recently deposited conglomerates, prior to the opening of the Rion Strait shortly after 400 ka (Gawthorpe et al., 2017).

6. Original fluvial flow of the pre-rift Mornos river to the south-south-west was blocked and buttressed by the newly formed Panachaikon fault and associated uplifted footwall, leading to the formation of the described alluvial fan and the diversion of drainage to the west and east into newly formed rift depocentres. In the present day, the south-flowing Mornos river forms a large delta that progrades south into the Gulf of Corinth.

7. Results from this research record the sedimentological expression of rift-basin evolution that cross-cuts an antecedent drainage network at a high angle. Three depositional models for this exist: (i) erosion through an uplifted footwall; (ii) diversion away from an uplifted footwall; (iii) deposition over the hangingwall dip-slope. While examples of each scenario can be found around the Gulf in the present day, here we show that intrabasinal faulting allows for the development of each scenario within the same basin segment as it evolves through time.

## 7. Acknowledgements

This research was funded by Aker BP, Anadarko, Areva (now Orano), BHP Billiton, Cairn India (Vedanta), Chevron, ConocoPhillips, Murphy Oil Corporation, Nexen-CNOOC, Saudi Aramco, Shell, Tullow Oil, Woodside and YPF, through their sponsorship of the Fluvial & Eolian Research Group at the University of Leeds. We are also grateful to our project partner Petrotechnical Data Systems (PDS) for support. We thank Ben Said and Rob Shuter for their assistance with field data collection. We thank reviewers Michael Hopkins, Bárbara Teixeira and Gary Axen, and Editor Cynthia Ebinger for their valuable comments and suggestions, which have significantly improved the manuscript.

## 8. References

- ABDUL AZIZ, H., SANZ-RUBIO, E., CALVO, J.P., HILGEN, F.J., & KRIJGSMAN, W. (2003) Palaeoenvironmental reconstruction of a middle Miocene alluvial fan to cyclic shallow lacustrine depositional system in the Calatayud Basin (NE Spain). *Sedimentology*, **50**, 211–236.
- ALLEN, J.R.L. (1982) Sedimentary structures: their character and physical basis. *Developments in Sedimentology*, **30**. Elsevier: Amsterdam.
- ALLEN, P.A., & DENSMORE, A.L. (2000) Sediment flux from an uplifting fault block. *Basin Res.*, **12**, 367–380.
- ALONSO-ZARZA, A.M. (2003) Palaeoenvironmental significance of palustrine carbonates and calcretes in the geological record. *Earth-Science Reviews*, **60**, 261-298.

- ALVAREZ-ZARIKIAN, C.A., SOTER, S., & KATSONOPOULOU, D. (2008) Recurrent Submergence and Uplift in the Area of Ancient Helike, Gulf of Corinth, Greece: Microfaunal and Archaeological Evidence. *Journal of Coastal Research*, **24**, 110–125.
- BACKERT, N., FORD, M., & MALARTRE, F. (2010) Architecture and sedimentology of the Kerinitis Gilbert-type fan delta, Corinth Rift, Greece. *Sedimentology*, **57**, 543–586.
- BECKERS, A., HUBERT-FERRARI, A., BECK, C., BODEUX, S., TRIPSANAS, E., SAKELLARIOU, D., & DE BATIST, M. (2015) Active faulting at the western tip of the Gulf of Corinth, Greece, from high-resolution seismic data. *Marine Geology*, **360**, 55–69.
- BELL, R.E., MCNEILL, L.C., BULL, J.M., HENSTOCK, T.J., COLLIER, R.E.L., & LEEDER, M.R. (2009) Fault architecture, basin structure and evolution of the Gulf of Corinth rift, central Greece. *Basin Research*, **21**, 824–855.
- BENTHAM, P., COLLIER, R.E., GAWTHORPE, R.L., LEEDER, M.R., & STARK, C. (1991) Tectono-sedimentary development of an extensional basin: the Neogene Megara Basin, Greece. *Journal of the Geological Society*, **148**, 923–934.
- BLAIR, T.C., & MCPHERSON, J.G. (1994) Alluvial Fans and their Natural Distinction from Rivers Based on Morphology, Hydraulic Processes, Sedimentary Processes, and Facies Assemblages. *SEPM Journal of Sedimentary Research*, **64A**, 450–489.
- CALHOUN, N.C., & CLAGUE, J.J. (2018) Distinguishing between debris flows and hyperconcentrated flows: an example from the eastern Swiss Alps. *Earth Surface Processes and Landforms*, **43**, 1280–1294.

- CHAKRABORTY, T., & GHOSH, P. (2010) The geomorphology and sedimentology of the Tista megafan, Darjeeling Himalaya: Implications for megafan building processes. *Geomorphology*, **115**, 252–266.
- CLARKE, L., QUINE, T.A., & NICHOLAS, A. (2010) An experimental investigation of autogenic behaviour during alluvial fan evolution. *Geomorphology*, **115**, 278–285.
- CLARKE, L.E. (2015) Experimental alluvial fans: Advances in understanding of fan dynamics and processes. *Geomorphology*, **244**, 135–145.
- COLLIER, R.E.L., & DART, C.J. (1991) Neogene to Quaternary rifting, sedimentation and uplift in the Corinth Basin, Greece. *Journal of the Geological Society*, **148**, 1049–1065.
- COLLIER, R.E.L., & GAWTHORPE, R.L. (1995) Neotectonics, drainage and sedimentation in central Greece: insights into coastal reservoir geometries in syn-rift sequences. *Geological Society, London, Special Publications*, **80**, 165–181.
- COLLINSON, J., MOUNTNEY, N.P., & THOMPSON, D. (2006) *Sedimentary structures*, 3<sup>rd</sup> edn, Terra Publishing, Harpenden.
- COLOMBERA, L., & BERSEZIO, R. (2011) Impact of the magnitude and frequency of debris-flow events on the evolution of an alpine alluvial fan during the last two centuries: Responses to natural and anthropogenic controls. *Earth Surface Processes and Landforms*, **36**, 1632–1646.
- COSTA, J.E. (1988) Rheologic, geomorphic, and sedimentologic differentiation of water floods, hyperconcentrated flows, and debris flows. In: *Flood geomorphology* (V.R.

Baker, R.C. Kochel and P.C. Patton, eds), 113-122. John Wiley & Sons, Inc.,  
Chichester.

CROCI, A., DELLA PORTA, G., & CAPEZZUOLI, E. (2016) Depositional architecture of a mixed travertine-terrigenous system in a fault-controlled continental extensional basin (Messinian, Southern Tuscany, Central Italy). *Sedimentary Geology*, **332**, 13–39.

CRONIN, S.J., LECOINTRE, J.A., PALMER, A.S., & NEALL, V.E. (2000) Transformation, internal stratification, and depositional processes within a channelised, multi-peaked lahar flow. *New Zealand Journal of Geology and Geophysics*, **43**, 117–128.

DART, C. J., COLLIER, R.E.L., GAWTHORPE, R.L., KELLER, J.V.A., & NICHOLS, G. (1994) Sequence stratigraphy of (?)Pliocene-Quaternary synrift, Gilbert-type fan deltas, northern Peloponnesos, Greece. *Marine and Petroleum Geology*, **11**, 545–560.

DAVIES, N.S., & GIBLING, M.R. (2010) Cambrian to Devonian evolution of alluvial systems: The sedimentological impact of the earliest land plants. *Earth-Science Reviews*, **98**, 171–200.

DEC, T. (1992) Textural characteristics and interpretation of second-cycle, debris-flow-dominant alluvial fans (Devonian of Northern Scotland). *Sedimentary Geology*, **77**, 269–296.

DEGNAN, P.J., & ROBERTSON, A.H.F. (1998) Mesozoic-early Tertiary passive margin evolution of the Pindos ocean (NW Peloponnese, Greece). *Sedimentary Geology*, **117**, 33–70.

- DENSMORE, A.L., ALLEN, P.A. & SIMPSON, G. (2007) Development and response of a coupled catchment fan system under changing tectonic and climatic forcing. *Journal of Geophysical Research*, **112**, F01002.
- DOUTSOS, T., KONTOPOULOS, N., & POULIMENOS, G. (1988) The Corinth-Patras rift as the initial stage of continental fragmentation behind an active island arc (Greece). *Basin Research*, **1**, 177–190.
- DOUTSOS, T., & PIPER, D.J.W. (1990) Listric faulting, sedimentation, and morphological evolution of the Quaternary eastern Corinth rift, Greece: First stages of continental rifting. *Bulletin of the Geological Society of America*, **102**, 812–829.
- ELIET, P.P., & GAWTHORPE, R.L. (1995) Drainage development and sediment supply within rifts, examples from the Sperchios basin, central Greece. *Journal of the Geological Society*, **152**, 883–893.
- ESU, D., & GIROTTI, O. (2015) The late Early Pleistocene non-marine molluscan fauna from the Synania Formation (Achaia, Greece), with description of nine new species (Mollusca: Gastropoda). *Archiv Für Molluskenkunde: International Journal of Malacology*, **144**, 65–81.
- FLOTTÉ, N., SOREL, D., MÜLLER, C., & TENSI, J. (2005) Along strike changes in the structural evolution over a brittle detachment fault: Example of the Pleistocene Corinth-Patras rift (Greece). *Tectonophysics*, **403**, 77–94.
- FORD, M., HEMELSDAËL, R., MANCINI, M., & PALYVOS, N. (2016) Rift migration and lateral propagation: evolution of normal faults and sediment-routing systems of the western Corinth rift (Greece). In: *The Geometry of Normal Faults* (Ed. By Childs C.,

- Holdsworth R.E., Jackson C.A-L., Manzcchi T., Walsh J.J., Yielding G.) Geological Society, London, Special Publications, (439) London.
- FORD, M., ROHAIS, S., WILLIAMS, E.A., BOURLANGE, S., JOUSSELIN, D., BACKERT, N., & MALARTE, F. (2013). Tectono-sedimentary evolution of the western Corinth rift (Central Greece). *Basin Research*, **25**, 3–25.
- FRANKE, D., HORNUNG, J., & HINDERER, M. (2015) A combined study of radar facies, lithofacies and three-dimensional architecture of an alpine alluvial fan (Illgraben fan, Switzerland). *Sedimentology*, **62**, 57–86.
- FROSTICK, L., & REID, I. (1989) Is structure the main control of river drainage and sedimentation in rifts? *Journal of African Earth Sciences*, **8**, 165–182.
- GAWTHORPE, R.L., FRASER, A.J., & COLLIER, R.E.L. (1994) Sequence stratigraphy in active extensional basins: implications for the interpretation of ancient basin-fills. *Marine and Petroleum Geology*, **11**, 642–658.
- GAWTHORPE, R., & COLELLA, A. (1990) Tectonic Controls on Coarse-Grained Delta Depositional Systems in Rift Basins. In: *Coarse-grained Deltas*, (Ed. By Colella A., Prior D.B.) International Association of Sedimentologists Special Publication, **10**, 113-127.
- GAWTHORPE, R.L., & LEEDER, M.R. (2000) Tectono-sedimentary evolution of active extensional basins. *Basin Research*, **12**, 195–218.
- GAWTHORPE, R.L., LEEDER, M.R., KRANIS, H., SKOURTSOS, E., ANDREWS, J.E., HENSTRA, G.A., MACK, G.H., MURAVCHIK, M., TURNER, J.A., & STAMATAKIS, M.

- (2017) Tectono-sedimentary evolution of the Plio-Pleistocene Corinth rift, Greece. *Basin Research*, **30**, 448–479.
- GLOPPEN, T.G., & STEEL, R.J. (1981) The deposits, internal structure and geometry in six alluvial fan-fan delta bodies (Devonian-Norway)-A study in the significance of bedding sequence in conglomerates. *Society for Sedimentary Geology Special Publication*, **31**, 49–69.
- GRAHAM, S.A., HENDRIX, M.S., JOHNSON, C.L., BADAMGARAV, D., BADARCH, G., AMORY, J., PORTER, M., BARSBOLD, R., WEBB, L.E., & HACKER, B.R. (2001) Sedimentary record and tectonic implications of Mesozoic rifting in southeast Mongolia. *Bulletin of the Geological Society of America*, **113**, 1560–1579.
- GUPTA, S., UNDERHILL, J.R., SHARP, I.R., & GAWTHORPE, R.L. (1999) Role of fault interactions in controlling synrift sediment dispersal patterns: Miocene, Abu Alaqa Group, Suez Rift, Sinai, Egypt. *Basin Research*, **11**, 167–189.
- HEMELSDAËL, R., FORD, M., MALARTRE, F., & GAWTHORPE, R.L. (2017) Interaction of an antecedent fluvial system with early normal fault growth: Implications for syn-rift stratigraphy, western Corinth rift (Greece). *Sedimentology*, **64**, 1957–1997.
- HOPKINS, M. C., & DAWERS, N. H. (2018) The role of fault length, overlap and spacing in controlling extensional relay ramp fluvial system geometry. *Basin Research*, **30**, 20–34.
- HWANG, I.G., CHOUGH, S.K., HONG, S.W., & CHOE, M.Y. (1995) Controls and evolution of fan delta systems in the Miocene Pohang Basin, SE Korea. *Sedimentary Geology*, **98**, 147–179.

- JO, H.R., RHEE, C.W., & CHOUGH, S.K. (1997) Distinctive characteristics of a streamflow-dominated alluvial fan deposit: Sanghori area, Kyongsang Basin (Early Cretaceous), southeastern Korea. *Sedimentary Geology*, **110**, 51–79.
- JO, H.R., & CHOUGH, S.K. (2001) Architectural analysis of fluvial sequences in the Northwestern part of Kyongsang Basin (Early Cretaceous), SE Korea. *Sedimentary Geology*, **144**, 307–334.
- KARPETA, W. P. (1993) Sedimentology and gravel bar morphology in an Archaean braided river sequence: the Witpan Conglomerate Member (Witwatersrand Supergroup) in the Welkom Goldfield, South Africa. *Geological Society, London, Special Publications*, **75**, 369–388.
- KIM, B.C., & LOWE, D.R. (2004) Depositional processes of the gravelly debris flow deposits, South Dolomite alluvial fan, Owens Valley, California. *Geosciences Journal*, **8**, 153–171.
- KHADKIKAR, A. S. (1999) Trough cross-bedded conglomerate facies. *Sedimentary Geology*, **128**, 39–49.
- KÖYKKÄ, J. (2011) Precambrian alluvial fan and braidplain sedimentation patterns: Example from the Mesoproterozoic Rjukan Rift Basin, southern Norway. *Sedimentary Geology*, **234**, 89–108.
- LEEDER, M.R., & JACKSON, J.A. (1993) The interaction between normal faulting and drainage in active extensional basins, with examples from the western United States and central Greece. *Basin Research*, **5**, 79–102.

- LEEDER, M.R., MARK, D.F., GAWTHORPE, R.L., KRANIS, H., LOVELESS, S., PEDENTCHOUK, N., SKOURTSOS, E., TURNER, J., ANDREWS, J.E., & STAMATAKIS, M. (2012) A “Great Deepening”: Chronology of rift climax, Corinth rift, Greece. *Geology*, **40**, 999–1002.
- LEWIS, M.M., JACKSON, C.A-L., & GAWTHORPE, R.L. (2017) Tectono-sedimentary development of early syn-rift deposits: the Abura Graben, Suez Rift, Egypt. *Basin Research*, **29**, 327–351.
- LINDSEY, D.A., LANGER, W.H., & KNEPPER JR., D.H. (2005) Stratigraphy, lithology, and sedimentary features of Quaternary alluvial deposits of the South Platte River and some of its tributaries east of the Front Range, Colorado. *U.S. Geological Survey Professional Paper 1705*.
- LOWE, D. R. (1979) Sediment gravity flows: their classification and some problems of application to natural flows and deposits. *SEPM Special Publication*, **27**, 75–82.
- MACK, G.H., & SEAGER, W.R. (1990) Tectonic control on facies distribution of the Camp Rice and Palomas Formations (Pliocene-Pleistocene) in the southern Rio Grande rift. *Bulletin of the Geological Society of America*, **102**, 45–53.
- MACK, G.H., JAMES, W.C., & MONGER, H.C. (1993) Classification of paleosols. *Geological Society of America Bulletin*, **105**, 129–136.
- MACK, G.H., & LEEDER, M.R. (1999) Climatic and tectonic controls on alluvial-fan and axial-fluvial sedimentation in the Plio-Pleistocene Palomas half graben, southern Rio Grande Rift. *Journal of Sedimentary Research*, **69**, 635–652.

- MAIZELS, J. (1993) Lithofacies variations within sandur deposits: the role of runoff regime, flow dynamics and sediment supply characteristics. *Sedimentary Geology*, **85**, 299–325.
- MAJOR, J.J. (1998) Pebble orientation on large, experimental debris-flow deposits. *Sedimentary Geology*, **117**, 151–164.
- MARTINI, I.P., & SAGRI, M. (1993) Tectono-sedimentary characteristics of Late Miocene-Quaternary extensional basins of the Northern Apennines, Italy. *Earth Science Reviews*, **34**, 197–233.
- MARTINS-NETO, M.A., & CATUNEANU, O. (2010) Rift sequence stratigraphy. *Marine and Petroleum Geology*, **27**, 247–253.
- MIALL, A.D. (1996) *The Geology of Fluvial Deposits, Sedimentary Facies, Basin Analysis, and Petroleum Geology*. Springer, New York, 582 pp.
- MIRABELLA, F., BUCCI, F., SANTANGELO, M., CARDINALI, M., CAIELLI, G., DE FRANCO, R., GUZZETTI, F., & BARCHI, M.R (2018) In press. Alluvial fan shifts and stream captures driven by extensional tectonics in central Italy. *Journal of the Geological Society*, **175**, 788-805.
- MORLEY, C.K., NELSON, R.A., PATTON, T.L., & MUNN, S.G. (1990) Transfer Zones in the East African Rift System and Their Relavance to Hydrocarbon Exploration in Rifts. *American Association of Petroleum Geologists Bulletin*, **74**, 1234–1253.

- MOSCARIELLO, A., MARCHI, L., MARAGA, F., & MORTARA, G. (2002) Alluvial fans in the Italian Alps: sedimentary facies and processes. *Flood Megaflood Process. Depos. Recent Anc. Examples*, **32**, 141–166.
- MURCIA, H.F., HURTADO, B.O., CORTÉS, G.P., MACÍAS, J.L., & CEPEDA, H. (2008) The ~ 2500 yr B.P. Chicoral non-cohesive debris flow from Cerro Machín Volcano, Colombia. *Journal of Volcanology and Geothermal Research*, **171**, 201–214.
- NEMEC, W., & STEEL, R.J. (1984) Alluvial and coastal conglomerates: their significant features and some comments on gravelly mass-flow deposits. *Sedimentology of Gravels and Conglomerates*, **10**, 1–31.
- NICHOLS, G.J., & FISHER, J.A. (2007) Processes, facies and architecture of fluvial distributary system deposits. *Sedimentary Geology*, **195**, 75–90.
- NIXON, C.W., MCNEILL, L.C., BULL, J.M., BELL, R.E., GAWTHORPE, R.L., HENSTOCK, T.J., CHRISTODOULOU, D., FORD, M., TAYLOR, B., SAKELLARIOU, D., FERENTINOS, G., PAPTAEODOROU, G., LEEDER, M.R., COLLIER, R.E.L., GOODLIFFE, A.M., SACHPAZI, M., & KRANIS, H. (2016) Rapid spatiotemporal variations in rift structure during development of the Corinth Rift, central Greece. *Tectonics*, **35**, 1225–1248.
- NORTH, C.P., & DAVIDSON, S.K. (2012) Unconfined alluvial flow processes: Recognition and interpretation of their deposits, and the significance for palaeogeographic reconstruction. *Earth-Science Reviews*, **111**, 199–223.
- ORI, G.G. (1989) Geologic history of the extensional basin of the Gulf of Corinth (?Miocene-Pleistocene), Greece. *Geology*, **17**, 918–921.

- PALYVOS, N., SOREL, D., LEMEILLE, F., MANCINI, M., PANTOSTI, D., JULIA, R.,  
TRIANANTAPHYLLOU, M., & DE MARTINI, P.-M. (2007) Review and new data on uplift  
rates at the W termination of the Corinth Rift and the NE Rion graben area (Achaia,  
NW Peloponnesos). *Bulletin of the Geological Society of Greece*, **40**, 412-424.
- PALYVOS, N., MANCINI, M., SOREL, D., LEMEILLE, F., PANTOSTI, D., JULIA, R.,  
TRIANANTAPHYLLOU, M., & DE MARTINI, P.-M. (2010). Geomorphological,  
stratigraphic and geochronological evidence of fast Pleistocene coastal uplift in the  
westernmost part of the Corinth Gulf Rift (Greece). *Geological Journal*, **45**, 78–104.
- PECHLIVANIDOU, S., COWIE, P.A., HANNISDAL, B., WHITTAKER, A.C., GAWTHORPE, R.L.,  
PENNOS, C. & RIISER, O.S. (2018) Source-to-sink analysis in an active extensional  
setting: Holocene erosion and deposition in the Sperchios rift, central Greece. *Basin  
Research*, **30**, 522-543.
- PIPER, D.J.W., KONTOPOULOS, N., ANAGNOSTOU, C., CHRONIS, G., & PANAGOS, A.G.  
(1990) Modern Fan Deltas in the Western Gulf of Corinth, Greece. *Geo-Marine  
Letters*, **10**, 5–12.
- PLATT, N.H., & KELLER, B. (1992) Distal alluvial deposits in a foreland basin setting—  
the Lower Freshwater Miocene, Switzerland: sedimentology, architecture and  
palaeosols. *Sedimentology*, **39**, 545–565.
- PUY-ALQUIZA, M.J., MIRANDA-AVILÉS, R., GARCÍA-BARRAGÁN, J.C., LOZA-AGUIRRE, I.,  
LI, Y., & ZANOR, G.A., (2017) Facies analysis, stratigraphic architecture and  
depositional environments of the Guanajuato conglomerate in the Sierra de  
Guanajuato, Mexico. *Boletín de La Sociedad Geológica Mexicana*, **69**, 385–408.

- READING, H.G. (1996) *Sedimentary Environments: Processes, Facies and Stratigraphy*, 3rd. Blackwell Scientific, Oxford.
- REITZ, M.D., & JEROLMACK, D.J. (2012) Experimental alluvial fan evolution: Channel dynamics, slope controls, and shoreline growth. *Journal of Geophysical Research: Earth Surface*, **117**, 1–19.
- RETALLACK, G.J. (2001) *Soils of the Past. An introduction to Paleopedology*. 2<sup>nd</sup> Ed. Blackwell Science, Oxford, 404pp.
- ROHAIS, S., ESCHARD, R., FORD, M., GUILLOCHEAU, F., & MORETTI, I. (2007a) Stratigraphic architecture of the Plio-Pleistocene infill of the Corinth Rift: Implications for its structural evolution. *Tectonophysics*, **440**, 5–28.
- ROHAIS, S., ESCHARD, R., & GUILLOCHEAU, F. (2008) Depositional model and stratigraphic architecture of rift climax Gilbert-type fan deltas (Gulf of Corinth, Greece). *Sedimentary Geology*, **210**, 132–145.
- SEGER, M., & ALEXANDER, J. (2009) Distribution of Plio-Pleistocene and Modern Coarse-Grained Deltas South of the Gulf of Corinth, Greece. *Tectonic Controls and Signatures in Sedimentary Successions*, **20**, 37–48.
- SHUKLA, U.K. (2009) Sedimentation model of gravel-dominated alluvial piedmont fan, Ganga Plain, India. *International Journal of Earth Sciences*, **98**, 443–459.
- SINCLAIR, I.K., SHANNON, P.M., WILLIAMS, B.P.J., HARKER, S.D., & MOOREN, J.G. (1994) Tectonic control on sedimentary evolution of three North Atlantic borderland Mesozoic basins<sup>1</sup>. *Basin Research*, **6**, 193–217.

- SKOURLIS, K., & DOUSOS, T. (2003) The Pindos Fold-and-thrust belt (Greece): Inversion kinematics of a passive continental margin. *International Journal of Earth Sciences*, **92**, 891–903.
- SOHN, Y.K., RHEE, C.W., & KIM, B.C. (1999) Debris Flow and Hyperconcentrated Flood-Flow Deposits in an Alluvial Fan, Northwestern Part of the Cretaceous Yongdong Basin, Central Korea. *The Journal of Geology*, **107**, 111–132.
- SOREL, D. (2000) A Pleistocene and still-active detachment fault and the origin of the Corinth-Patras rift, Greece. *Geology*, **28**, 83–86.
- STEEL, R.J., & THOMPSON, D.B. (1983) Structures and textures in Triassic braided stream conglomerates (“Bunter” Pebble Beds) in the Sherwood Sandstone Group, North Staffordshire, England. *Sedimentology*, **30**, 341–367.
- SURESH, N., BAGATI, T.N., KUMAR, R., & THAKUR, V.C. (2007) Evolution of quaternary alluvial fans and terraces in the intramontane Pinjaur Dun, Sub-Himalaya, NW India: Interaction between tectonics and climate change. *Sedimentology*, **54**, 809–833.
- TEIXEIRA, B.M.N., ASTINI, R.A., GOMEZ, F.J., MORALES, N., & PIMENTEL, M.M. (2018). Source-to-sink analysis of continental rift sedimentation: Triassic Cuyo basin, Precordillera Argentina. *Sedimentary Geology*, **376**, 164–184.
- TODD, S.P. (1989) Stream-driven, high-density gravelly traction carpets: possible deposits in the Trabeg Conglomerate Formation, SW Ireland and some theoretical considerations of their origin. *Sedimentology*, **36**, 513–530.

- TURNER, S.A. (2010) Sedimentary record of Late Neoproterozoic rifting in the NW Tarim Basin, China. *Precambrian Research*, **181**, 85–96.
- UNDERHILL, J.R. (1989) Late Cenozoic deformation of the Hellenic foreland, Western Greece. *Bull. Geol. Soc. Am.*, **101**, 613–634.
- VAN DIJK, M., KLEINHANS, M.G., POSTMA, G., & KRAAL, E. (2012) Contrasting morphodynamics in alluvial fans and fan deltas: Effect of the downstream boundary. *Sedimentology*, **59**, 2125–2145.
- WELLS, N.A. (1984) Sheet debris flow and Sheetflood conglomerates in Cretaceous cool-maritime alluvial fans, South Orkney Islands, Antarctica. *Sedimentology of Gravels and Conglomerates*, **10**, 133-145.
- WENT, D.J. (2005) Pre-vegetation alluvial fan facies and processes: An example from the Cambro-Ordovician Rozel Conglomerate Formation, Jersey, Channel Islands. *Sedimentology*, **52**, 693–713.
- ZELILIDIS, A. (2000) Drainage evolution in a rifted basin, Corinth graben, Greece. *Geomorphology*, **35**, 69–85.

### **Figure and table captions**

**Table 1.** Descriptions and interpretations of studied lithofacies. Facies codes are based on the following pattern; (largest grain size; B, C, P, G, S, F) – (sorting; w – well, r –

moderate, p – poor)(clast packing; t – tight, l – loose)(structures; m – massive, f – fining up, l – sand lenses, c – cement, e – conglom. lenses, h – horizontal stratification).

**Fig. 1.** Map of the study area and the Gulf of Corinth rift, adapted from Gawthorpe et al. (2017). (A) Map of the entire Corinth Rift detailing distributions of syn-rift sediments and pre-rift basement. Active faults and inactive faults are represented in red and black colours respectively. Fault mapping is defined from Rohais et al. (2007a), Ford et al. (2013, 2016), Gawthorpe et al., (2017). (B) Detailed map of the study area for this paper showing the mapped extent of the Rodini, Salmoniko and Synania Fms., and study sites used in this research.

**Fig. 2.** Images detailing data collection methods at 3 different scales (tens of metres, metres, and centimetre scale). Integration of datasets in this study allows for the underpinning of larger scale regional variations by higher-resolution facies and individual clast analyses (where ‘a’, ‘b’ and ‘c’ represent clast long, intermediate, and short axes respectively).

**Fig. 3.** (A) Study area map displaying regional variations in stratigraphic dip and dip direction. Note the approximate radial pattern of dips away from the north of the study area. (B) Approximate areas of time slices through the study area between relatively older, middle-aged and younger stratigraphy. Lines of section A-A’, B-B’, C-C’, D-D’ are located. (C) Fence diagram of structural cross sections through study area.

**Fig. 4.** Regional logs detailing lithological variations over the study area. Note the increase of conglomeratic facies both up-section (towards the end of the deposition of the Rodini Fm.) and towards the west and north.

**Fig. 5.** Outcrop images of each of the 15 facies detailed in Table 1. Arrows represent 1 m scale and indicate younging direction.

**Fig. 6a.** Sedimentary logs of the Rodini Fm. and Salmoniko Fm. deposited during rift initiation (vertical scale in metres). Initial sheet-like mass flows (AE3 in L1) close to the fan apex transition downstream into persistent non-cohesive debris flows and intermittent sand-laden hyperconcentrated flows (AE1 and AE2 in L2). Further to the east, finer grained facies dominate in distal locations (L3, L4, L5) with intermittent active lobe deposition represented by coarse debris-flow conglomerates (L6). See Fig. 3 for inset map definition.

**Fig. 6b.** Sedimentary logs of the Rodini Fm. deposited after rift initiation (vertical scale in metres). Coarse conglomerates close to the fan apex (L7, L8, L9) extend further into the basin than during rift initiation. These transition laterally into finer grained facies on inactive lobes (L10) and recently active lobes (L11, L12, L13). Pedogenic development in L12 combined with frequent conglomerate horizons (formed under upper flow regime) indicate frequent lobe switching. See Fig. 3 for inset map definition.

**Fig. 6c.** Sedimentary logs of the Rodini Fm. during its final phase of deposition before lacustrine transgression (vertical scale in metres). Coarse debris-flow conglomerates sourced from the north dominate deposition across the study area (L14, L19, L20) with

smaller fans sourced from the uplifted footwall in the south developed (L16, L18, L19). L15 represents the lacustrine transgression and prolonged activity on the Psathopyrgos fault. See Fig. 3 for inset map definition.

**Fig. 7.** 3D architectural element models displaying vertical and lateral nature of individual elements, and interpretations of their depositional processes. Yellow arrows indicate dominant sediment transport direction.

**Fig. 8.** Diagram displaying lithological variations across the study area through time. The tectonostratigraphic record shows the progradational nature of the hangingwall-sourced fan and of smaller, footwall-sourced fans through times before lacustrine transgression. Relative timings are detailed in Palyvos et al. (2007).

**Fig. 9.** Palaeocurrent map showing directions of palaeoflow across the study area through time. Persistent flow to the west and east (with a southerly influence) indicate diversion of the alluvial system into axial depocentres in the rift. Small-scale fans sourced over the uplifted footwall are indicated by northerly dominated flow during late-phase deposition.

**Fig. 10.** Palaeoenvironmental reconstruction of the Panachaikon-Psathopyrgos fault block through time, from 2 Ma – present day. Faulting initially cut through the pre-rift Hellenide thrust-and-fold belt, with uplifted footwalls blocking fluvial flow to the southwest and forming an alluvial fan and associated axial fluvial systems (Rodini Fm. and Salmoniko Fm.). Initiation of the Psathopyrgos fault cut off sediment supply from

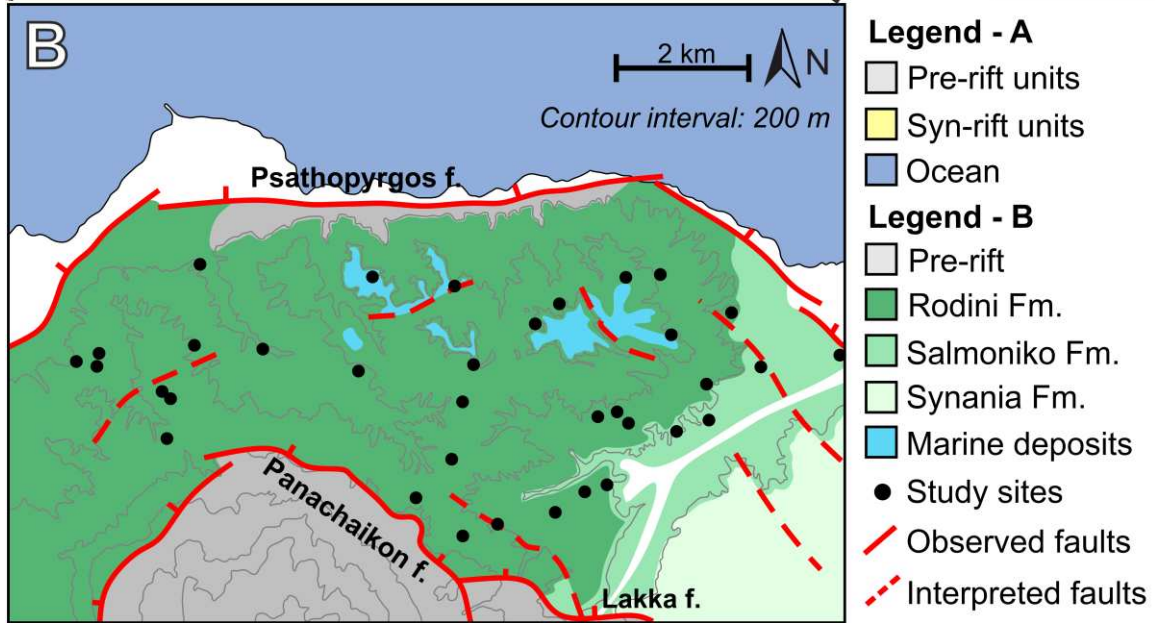
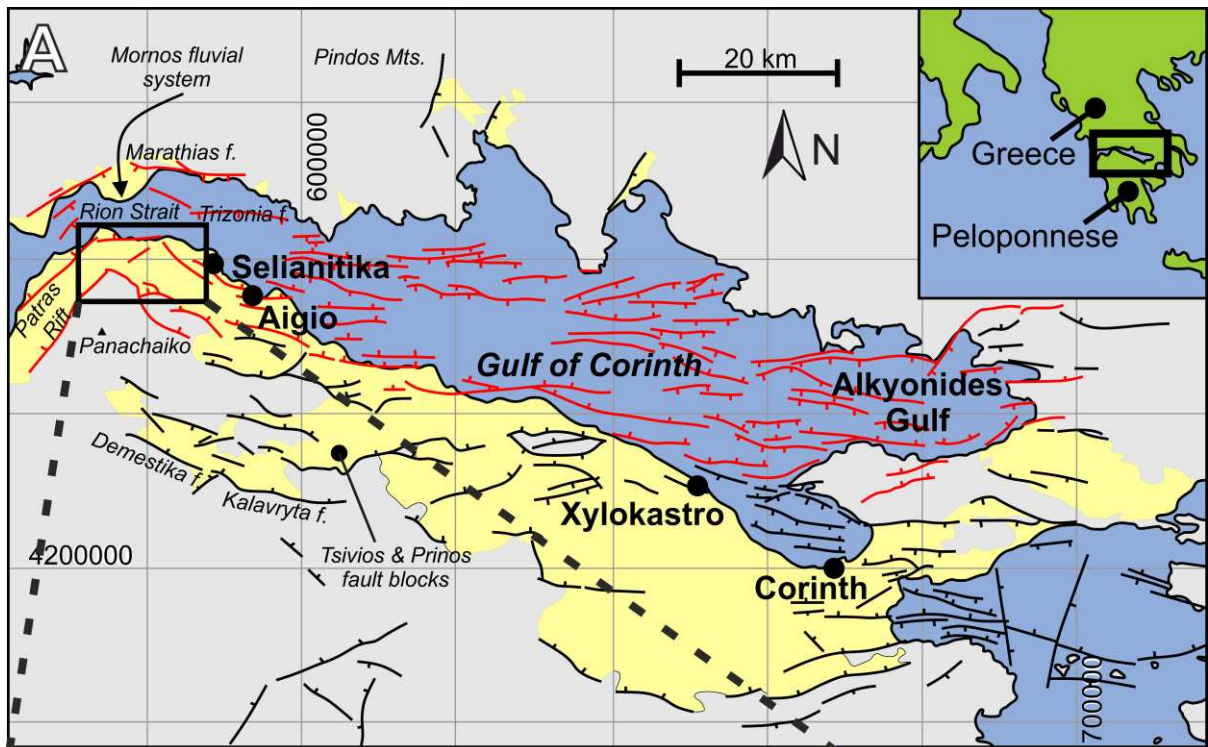
the north, causing a lacustrine transgression and the backstepping of a major delta up the hangingwall dip slope.

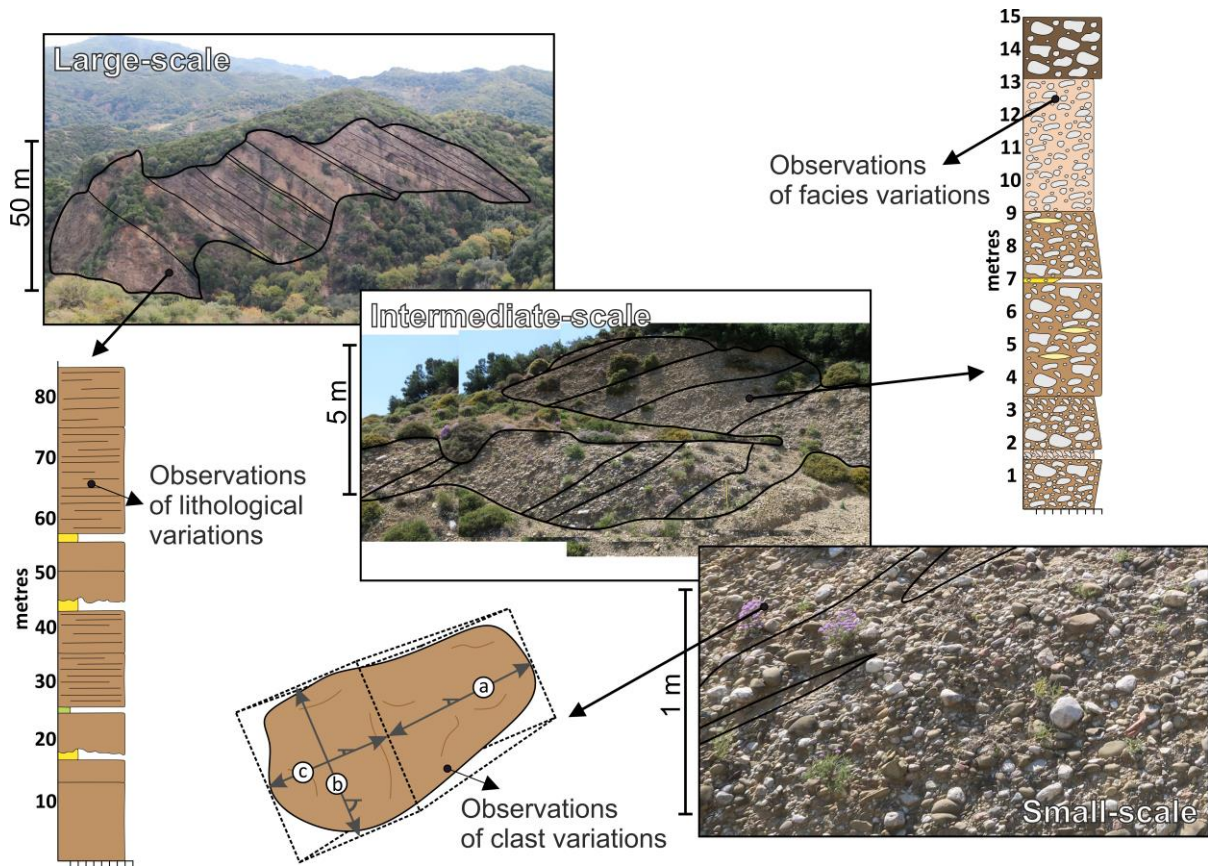
Code	Lithofacies	Description	Interpretation
B-wtm	Well-sorted boulder conglomerate	Clearly bedded, clast-supported (90-100%), with granule matrix. Tightly packed with sub-rounded to sub-angular clasts up to 50 cm in diameter. Form massive beds with erosional bases.	Conglomeratic debris-flow deposits proximal to the sediment source at the apex of an alluvial fan. More consistent, high-energy flows represented by tight packing of boulders and their large sizes (Puy-Alquiza et al., 2017, Teixeira et al., 2018).
B-rlf	Moderately-sorted normally graded boulder conglomerate	Clearly bedded, clast-supported (80-100%), with medium-coarse sand matrix. Loosely packed with rounded-sub-rounded clasts up to 30 cm in diameter. Normally grade to granule-pebble clasts and have erosive bases.	Bedload stream deposits in the upper-fan to mid-fan transition, close to fan apex, with discrete units formed by stream avulsions Fining upward grain-size trend and imbrication indicate turbulent nature of flow. (Moscariello et al., 2002; Reitz & Jerolmack, 2012).
B-plm	Poorly-sorted boulder conglomerate	Clearly bedded, clast-supported (80-90%), with medium sand-granule matrix. Loosely packed with sub-rounded to sub-angular clasts up to 50 cm in diameter. Form massive beds, may have erosive bases.	Non-cohesive debris flow deposits in the mid-fan represented by an increased matrix proportion and lack of sorting, indicating single event deposits. Further supported by erosive bases to units. (Murcia et al., 2008, Colombera & Bersezio, 2011).
B-pll	Poorly-sorted boulder conglomerate with sand lenses	Crudely bedded, clast-supported (70-90%) with medium-coarse sand matrix. Loosely packed with rounded to sub-angular clasts up to 30 cm in diameter. Beds contain medium sand lenses.	Non-cohesive debris flow deposits close to the fan toe. Higher matrix proportions and sand lenses represent a decrease in energy, either in distal locations or as trails behind transported clasts. (Kim et al., 2009; Shukla, 2009).
B-plc	Poorly-sorted boulder conglomerate with strong cement	Crudely bedded, clast-supported (70-90%) with well cemented medium sand-granule matrix. Loosely packed with sub-rounded to sub-angular clasts up to 30 cm in diameter. Form massive beds.	Cemented debris flow deposits, predicted to have experienced dissolution of carbonate clasts and subsequent reprecipitation, common in other areas of the Gulf of Corinth. (Backert et al., 2010; Gawthorpe et al., 2017).

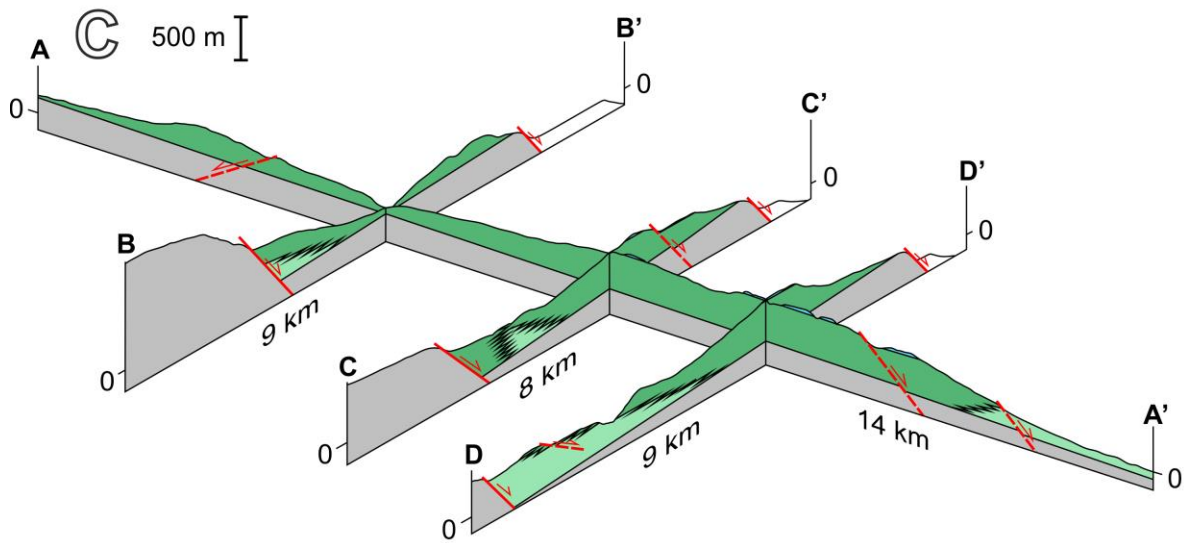
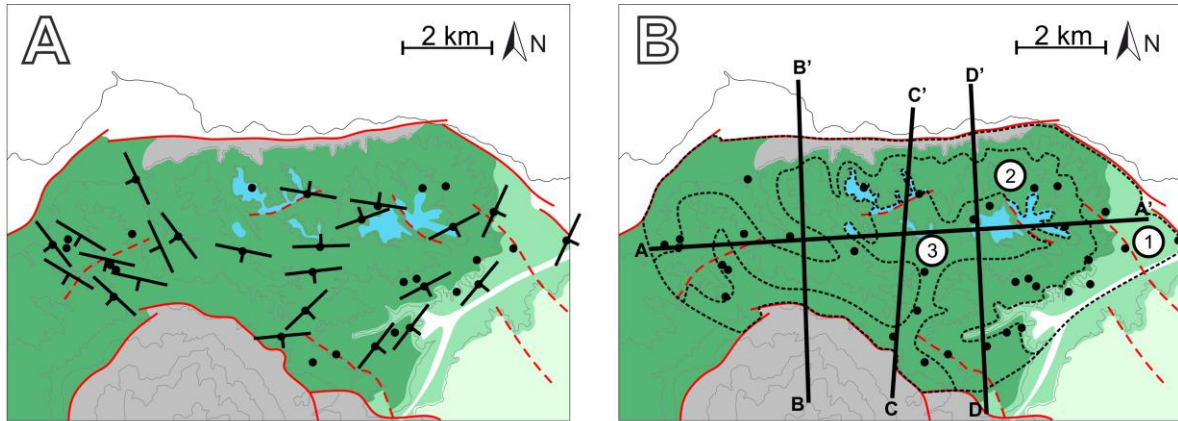
B-ple	Poorly-sorted, polymodal boulder conglomerate	Crudely bedded, clast-supported (90%) with medium sand-granule matrix. Loosely packed with rounded to sub-angular clasts up to 30 cm in diameter. Contains coarser and finer discontinuous lenses in each unit.	Streamflow deposits represented by highly variable flows leading to the interbedding of finer and coarser clast-supported, clean conglomerate lenses, forming low-relief bars. (Karpeta, 1993; Kim et al., 2009).
C-rl1	Moderately-sorted cobble conglomerate	Clearly bedded, clast supported (80-90%) with medium-coarse sand matrix. Loosely packed with rounded-sub-angular clasts up to 15 cm in diameter. Form massive beds. Some discontinuous sand lenses.	Debris-flow deposits close to the fan toes, finer grain sizes represent lower energy compared to B-pll. Sand lenses represent poorly developed flood dune bar deposits. (Lindsey et al., 2005; Chakraborty & Ghosh, 2010).
C-pt1	Poorly-sorted, horizontally stratified cobble conglomerate	Crudely bedded, clast-supported (80-90%) with medium-coarse sand matrix. Tightly packed with rounded to sub-angular clasts up to 15 cm in diameter. Beds are horizontally stratified.	Cobble bedload sheet deposits in the upper-fan to mid-fan transition as a result of turbulent flash flood flows, creating horizontal stratification. (Moscariello et al., 2002; Teixeira et al., 2018).
P-wtm	Well-sorted pebble conglomerate	Clearly bedded, clast-supported (90-100%) with medium sand matrix. Tightly packed with sub-rounded clasts up to 5 cm in diameter. Form massive beds of texturally mature clasts.	Relatively low-energy streamflow bedload deposits. Flow is consistent leading to clean, well-sorted fine grained conglomerates. Deposited away from large fan toe, or more proximally on a smaller alluvial fan. (Steel & Thompson, 1983; Ford et al., 2016).
G-wtm	Well-sorted granule conglomerate	Clearly bedded, clast-supported (90-100%) with medium sand matrix. Tightly packed with sub-rounded clasts up to 1 cm in diameter. Form massive beds of texturally mature clasts.	Relatively very low energy streamflow bedload deposits. Flows wash away silt and clay particulates, leading to clean, very well-sorted fine-grained conglomerates. (Steel & Thompson, 1983; Ford et al., 2016).
S-l	Massive silty sandstone with granule-cobble lenses	Crudely bedded, poorly-sorted silt to coarse grade sand. Intermittent well-sorted granule to cobble grade lenses throughout.	Rapid finer-grained sediment dumping from suspension in flows, with periods of high energy allowing upper plane-bed conglomerate deposition. (Lindsey et al., 2005; Franke et al., 2015).

S-s	Massive silty sandstone with intermittent clasts	Crudely bedded, poorly-sorted silt to coarse grade sand. Single clasts present randomly throughout massive beds, up to 2 cm in diameter.	Deposited in the most distal portions of a hyperconcentrated flow, where energy can only sustain rare small clasts. Rapid deposition from suspension. (Wells, 1984, Franke et al., 2015)
S-h	Silty sandstone with horizontal laminations	Crudely bedded, poorly-sorted silt to coarse grade sand. Horizontally laminated picking out fine grained sections, laminations typically 3-5 mm apart and increase in frequency up-section.	Waning debris flows or streamflow deposit laminated sands and silts away from main channel flow locations. (Allen, 1982; Colombera & Bersezio, 2011).
S-sh	Massive silty sandstone with shell fragments	Crudely bedded, poorly-sorted silt to coarse grade sand. Contain shell fragments up to 0.5-1 cm diameter that are present randomly or in thin < 15 cm laterally discontinuous lenses.	Low-moderate energy shallow lacustrine deposits where fragile shells are broken up by small amounts of current and wave action. (Alvarez-Zarikian et al., 2008; Ford et al., 2016).
F	Fine grained mudstone	Clearly bedded, well sorted clay-mud grade unit. Light to dark grey, brown, and cream colours present. Highly fissile with no structure, form laterally continuous beds up to 10 cm thick.	Overbank palaeosol development representing areas away from the influence of floods and channel processes. (Lindsey et al., 2005; Franke et al., 2015).

---

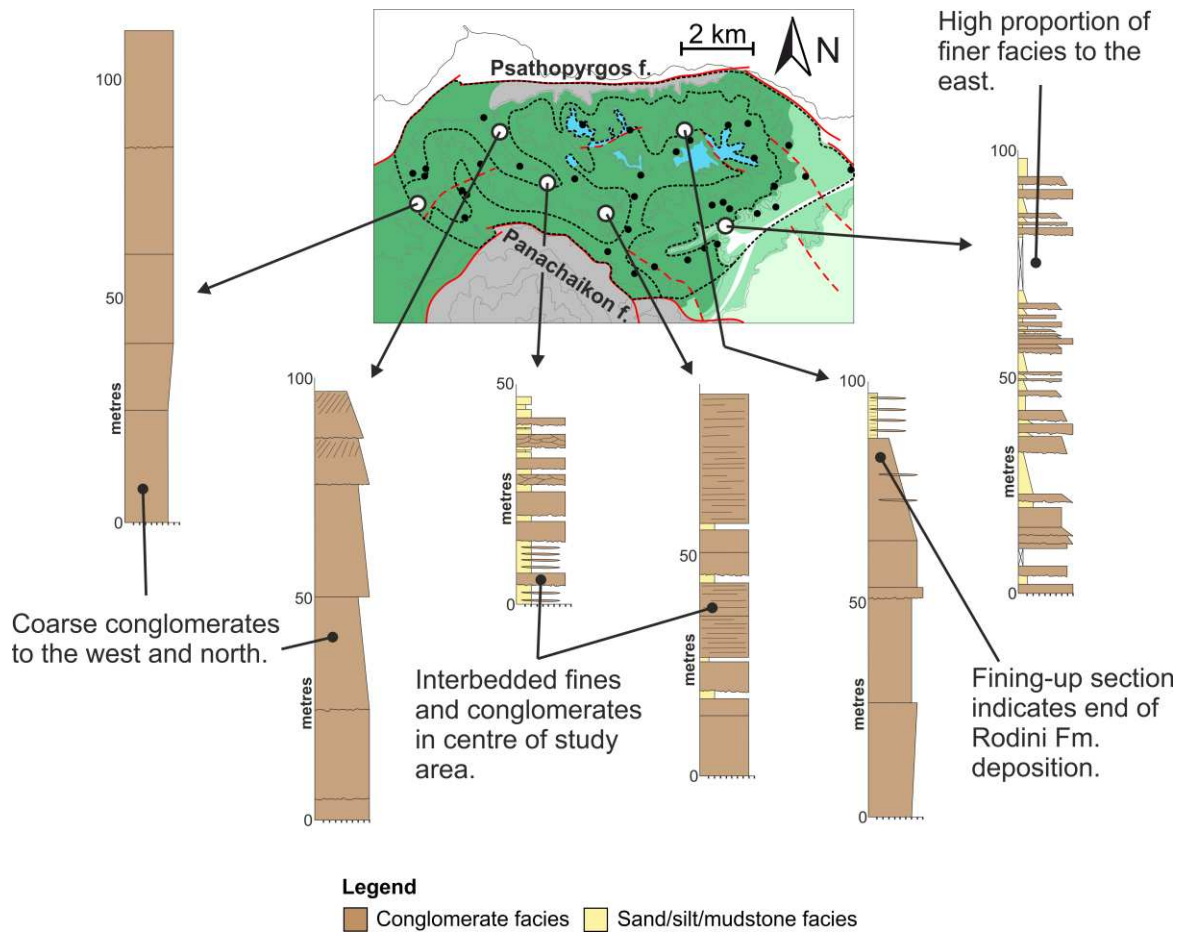




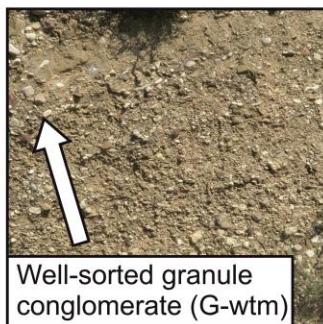
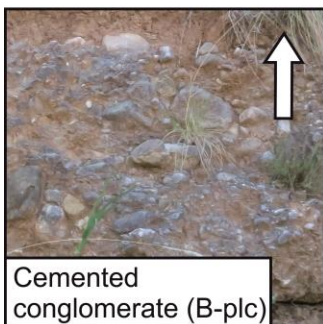
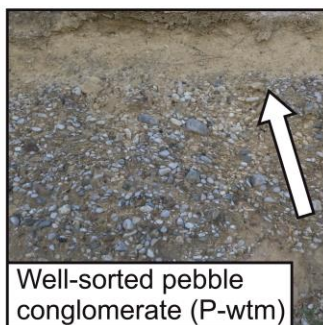
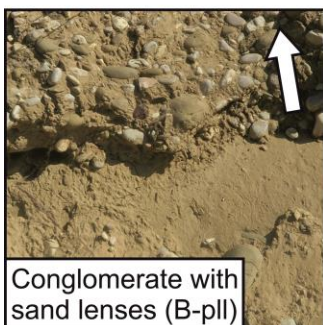
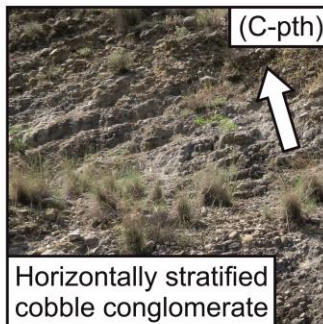
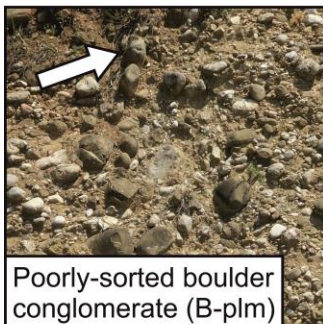
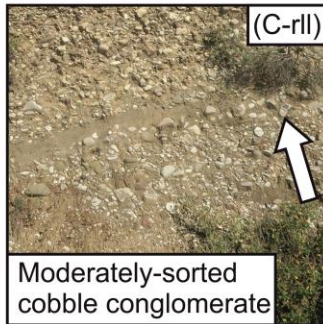
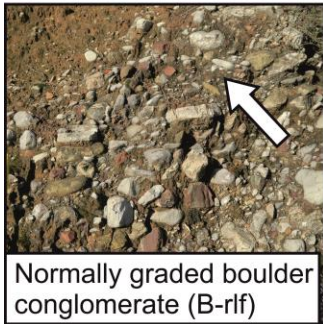
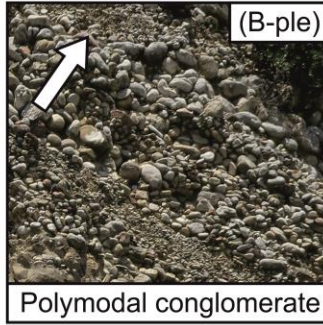
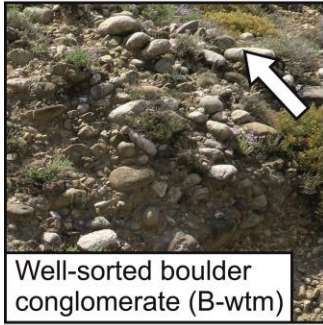


**Legend**

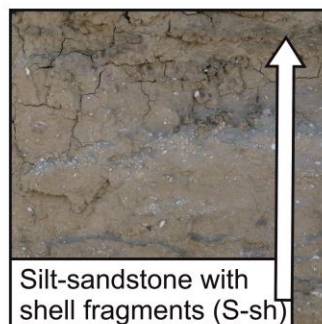
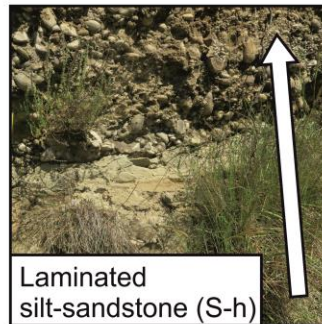
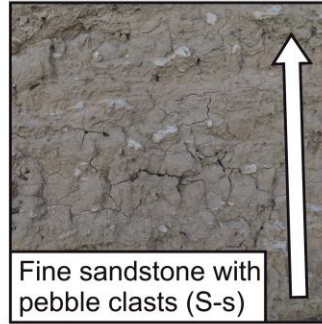
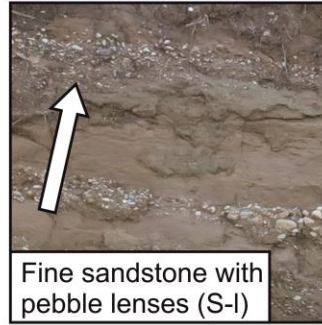
- |               |                 |                      |                   |
|---------------|-----------------|----------------------|-------------------|
| Pre-rift      | Synania Fm.     | Observed faults      | Youngest deposits |
| Rodini Fm.    | Marine deposits | Interpreted faults   | ↑                 |
| Salmoniko Fm. | Study sites     | Strike/dip direction | Oldest deposits   |



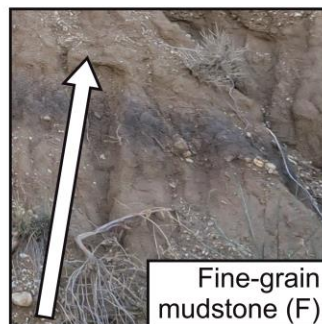
**Conglomerate facies**



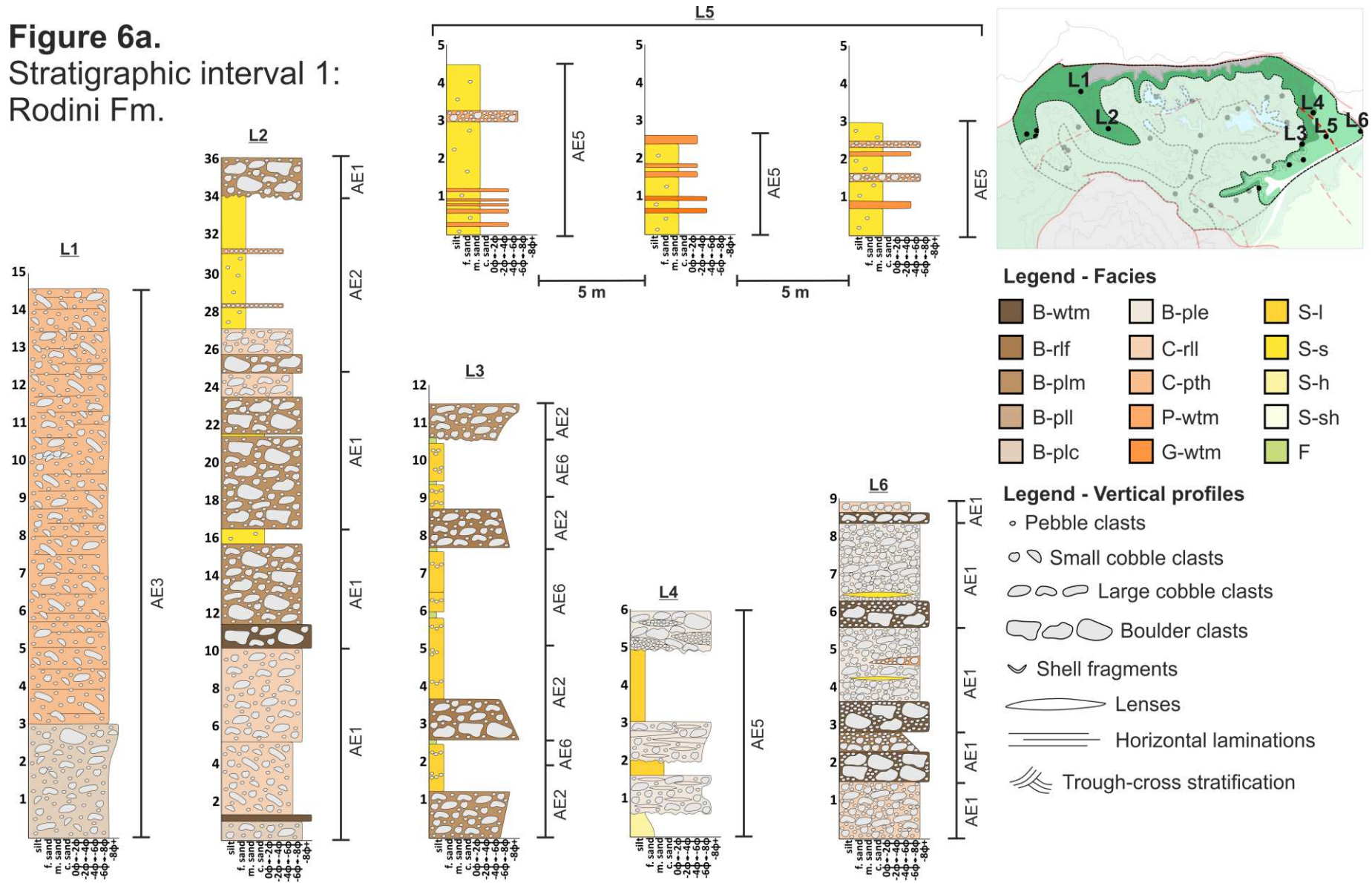
**Silt/sand-grade facies**



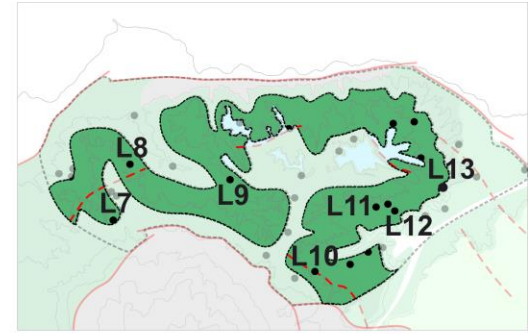
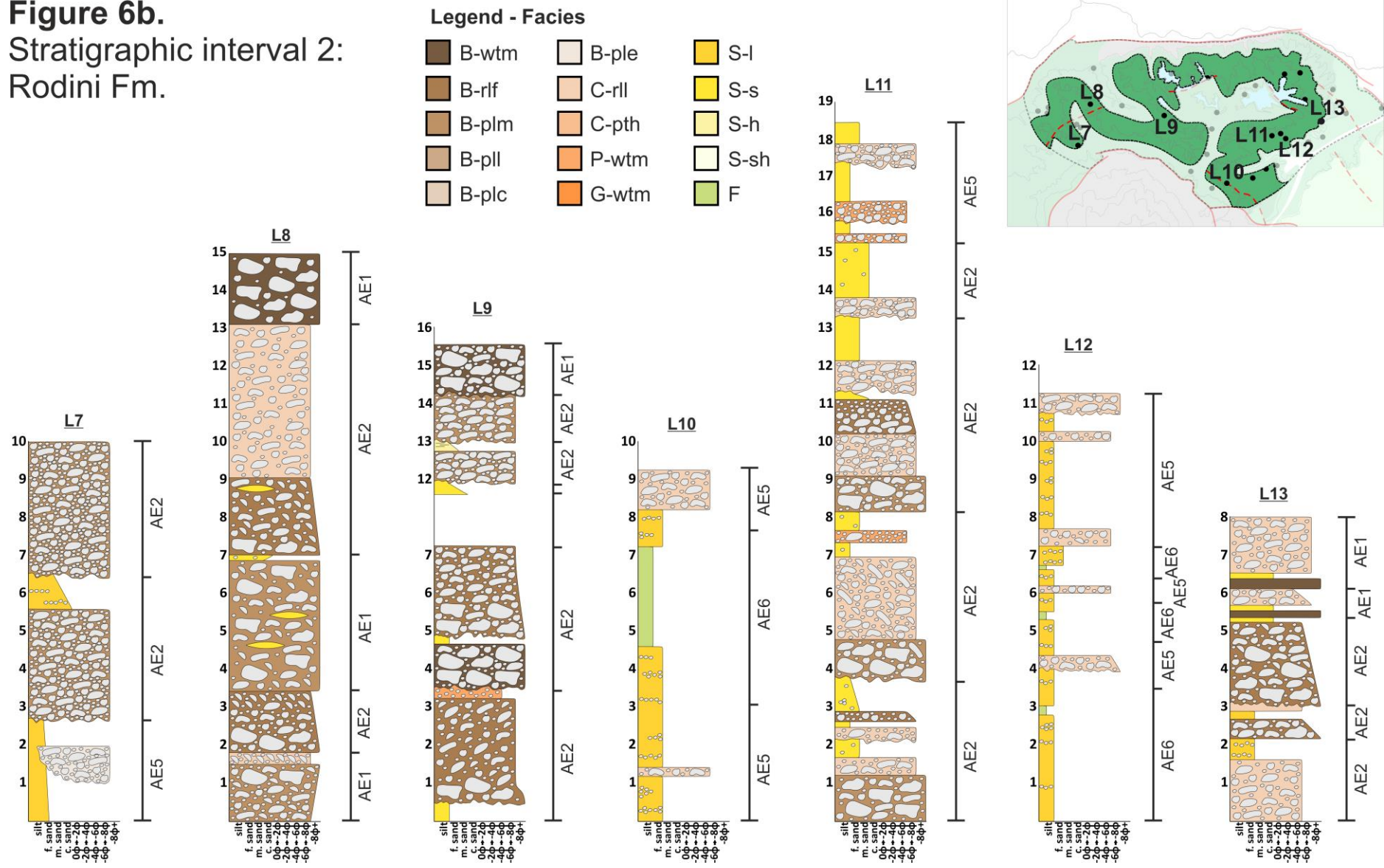
**Clay-grade facies**



**Figure 6a.**  
Stratigraphic interval 1:  
Rodini Fm.

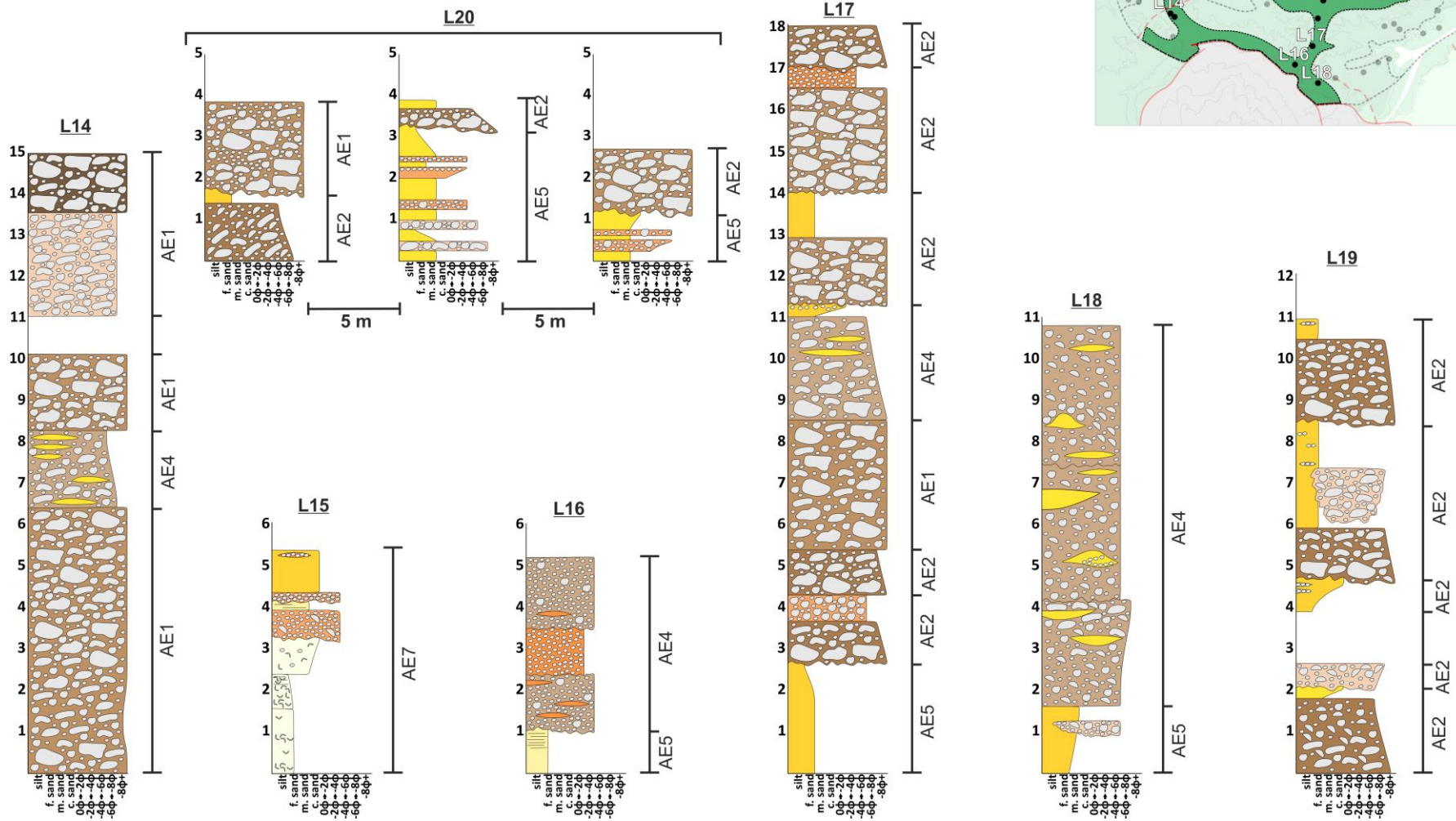
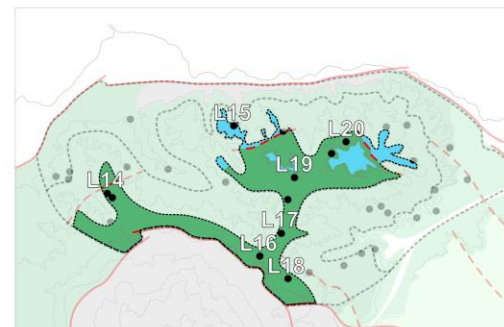
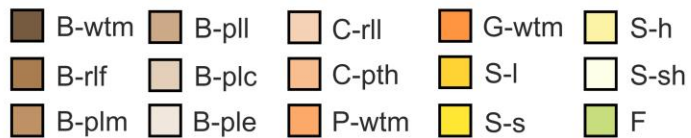


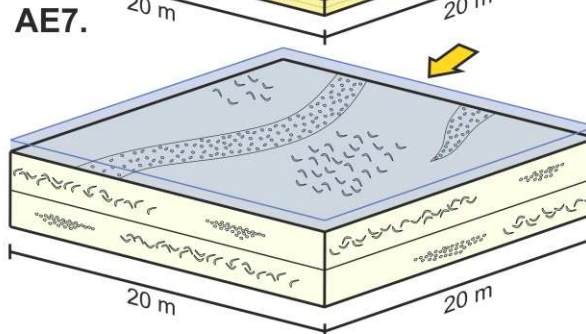
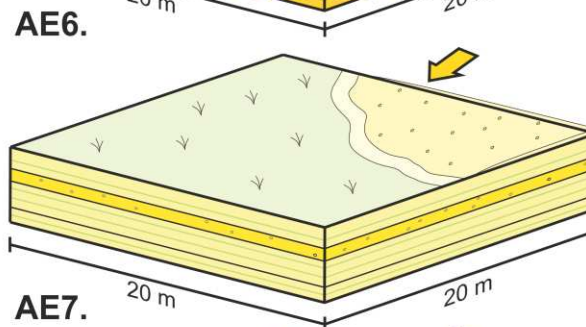
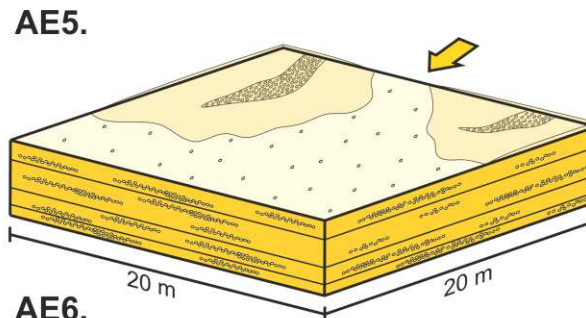
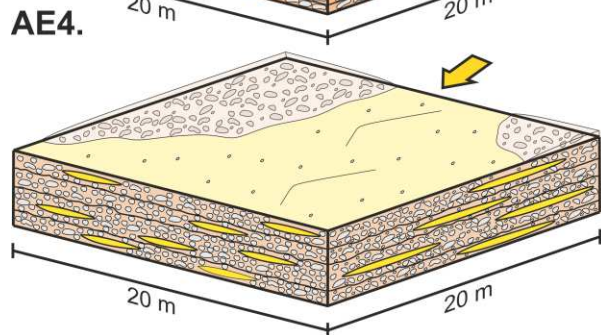
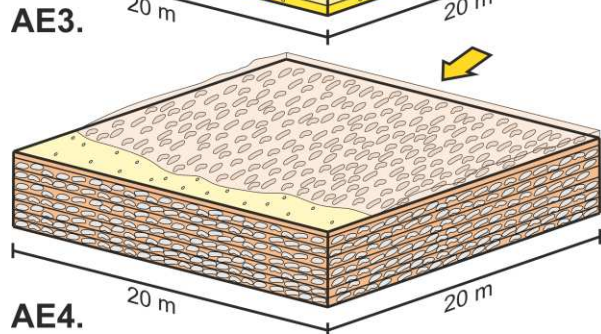
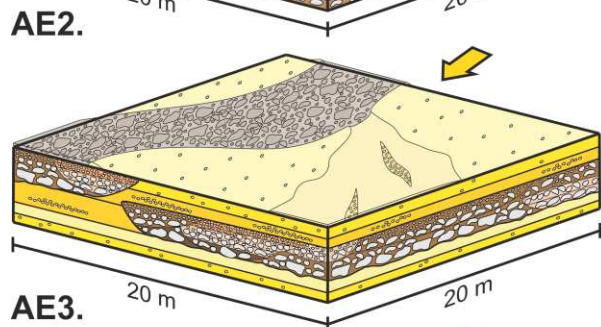
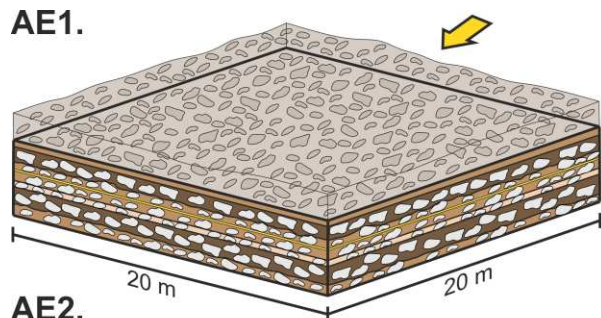
**Figure 6b.**  
Stratigraphic interval 2:  
Rodini Fm.



**Figure 6c.**  
 Stratigraphic interval 3:  
 Rodini Fm. & Lacustrine Sands

**Legend - Facies**



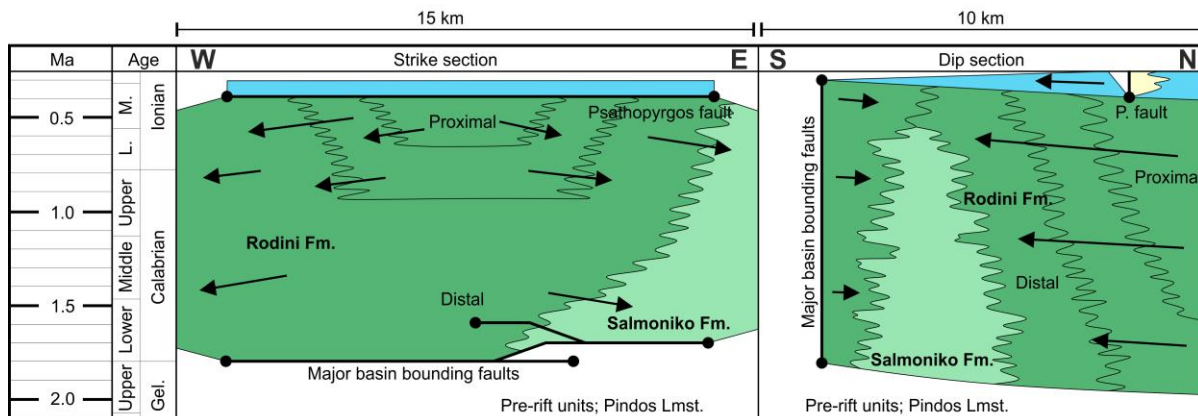
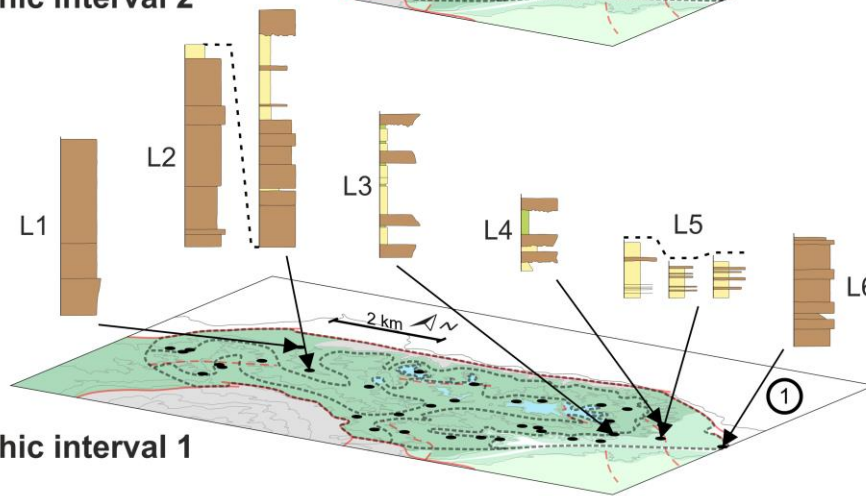
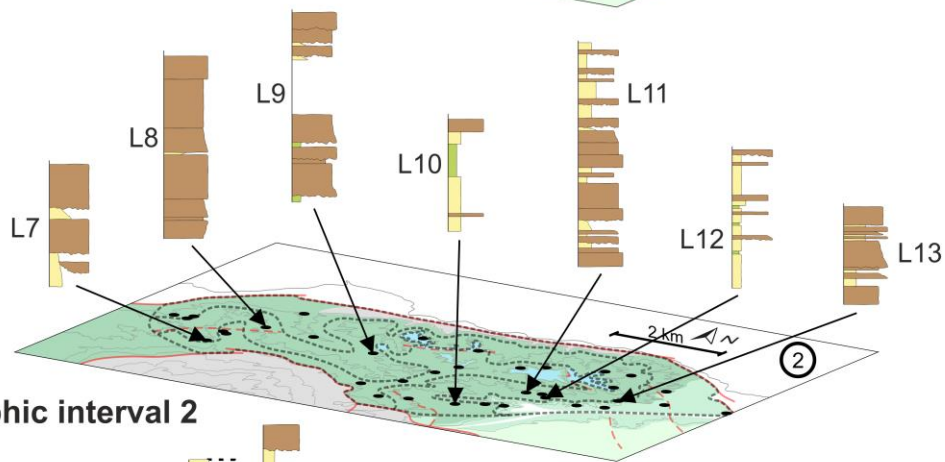
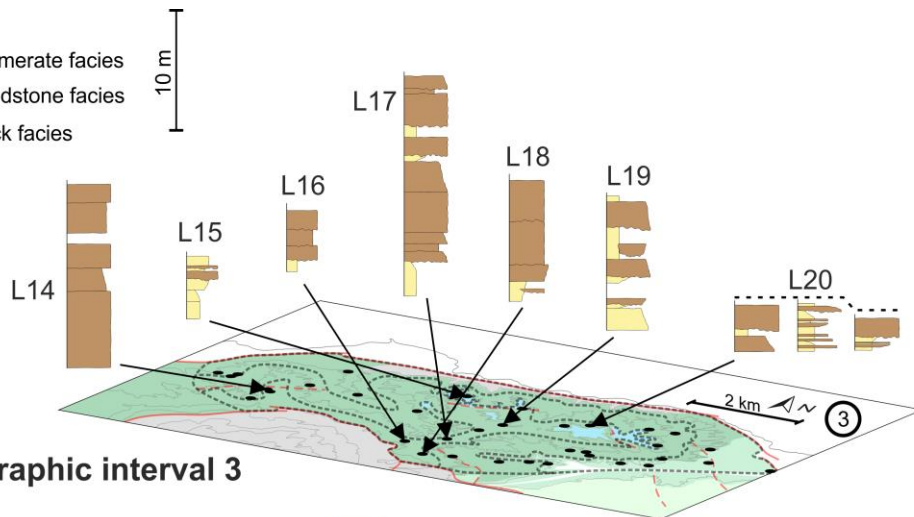


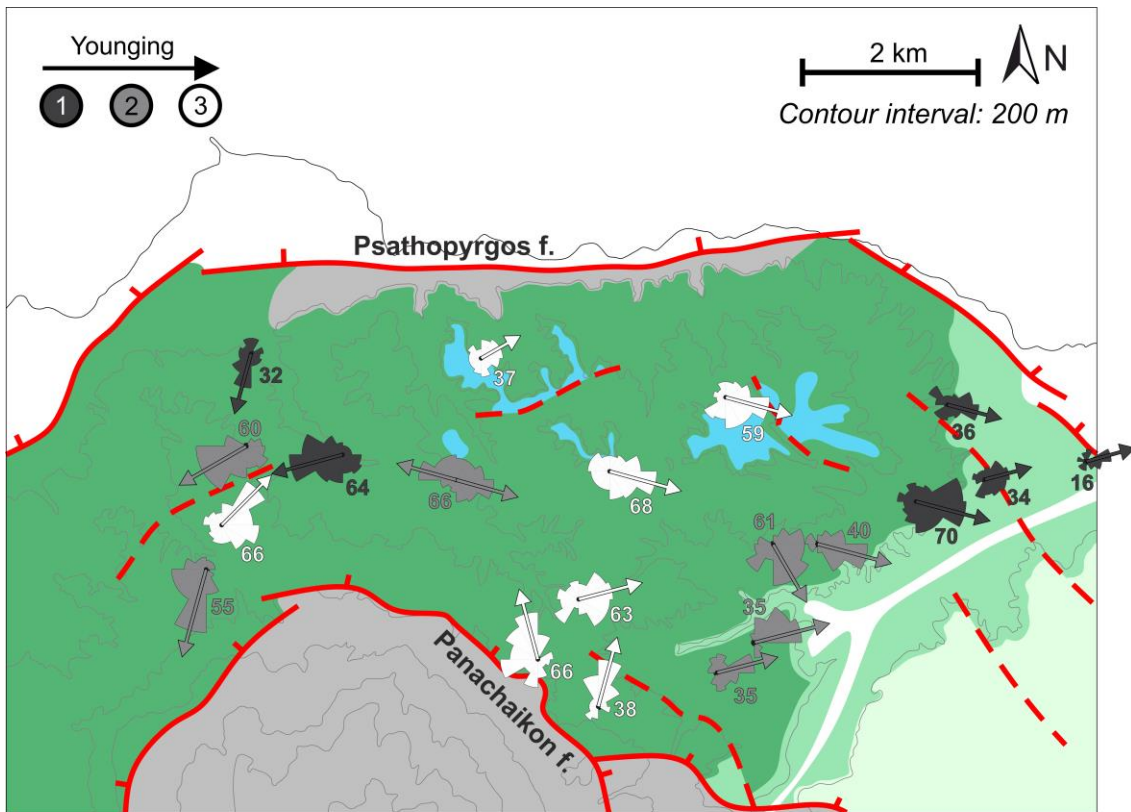
**Legend**

B-wtm	B-ple	S-l	Pebble clasts
B-rlf	C-rlf	S-s	Large cobble clasts
B-plm	C-ptm	S-h	Boulder clasts
B-pll	P-wtm	S-sh	Shell fragments
B-plc	G-wtm	F	Lenses

**Legend**

- Conglomerate facies
- Silt/sandstone facies
- Mudrock facies





**Legend**

- |            |               |                 |                    |
|------------|---------------|-----------------|--------------------|
| Pre-rift   | Salmoniko Fm. | Marine deposits | Observed faults    |
| Rodini Fm. | Synania Fm.   | Study sites     | Interpreted faults |

